Title: News from the ultra-high energy cosmic ray sky

Date: Dec 12, 2017 11:00 AM

URL: http://pirsa.org/17120007

Abstract: <p>After more than 12 years of continuous data taking, the Pierre Auger Observatory has collected the largest dataset of ultra-high energy cosmic rays (UHECR) to date. The results obtained in the last years include, for example, precise and accurate measurements of the UHECR flux across a few decades in energy, revealing distinctive spectral features that can bring valuable information on different astrophysical processes like: the transition from galactic to extragalactic fluxes; the different energy loss processes to which ultra-relativistic charged particles are subject during their propagation; the energetics of the production and acceleration of particles at the candidate sources. In this talk, I should however focus on a particular observational probe, that is, the small levels of anisotropy in the flux of UHECR at different angular scales: from the small and intermediate ones, important for the identification of possible point sources, to the large angular scales, usually used to search for signs of the galactic to extragalactic transition. In particular, special attention will be devoted to the first observation of a large scale anisotropy signal at energies above 8x10^18 eV recently reported by the collaboration.</p>

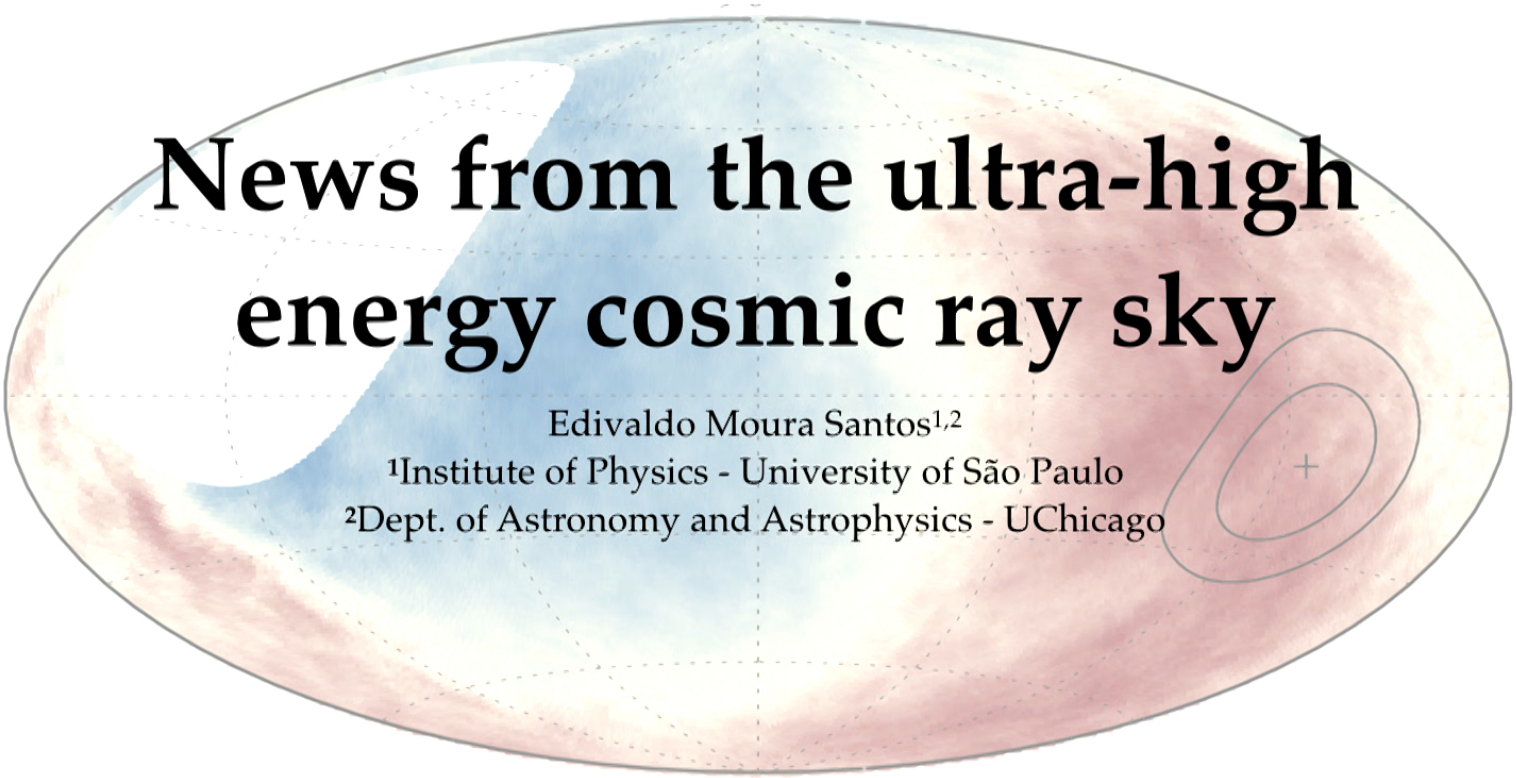

News from the ultra-high energy cosmic ray sky

Edivaldo Moura Santos[1,2]
[1]Institute of Physics - University of São Paulo
[2]Dept. of Astronomy and Astrophysics - UChicago

PI cosmology seminar, December 12, 2017

1

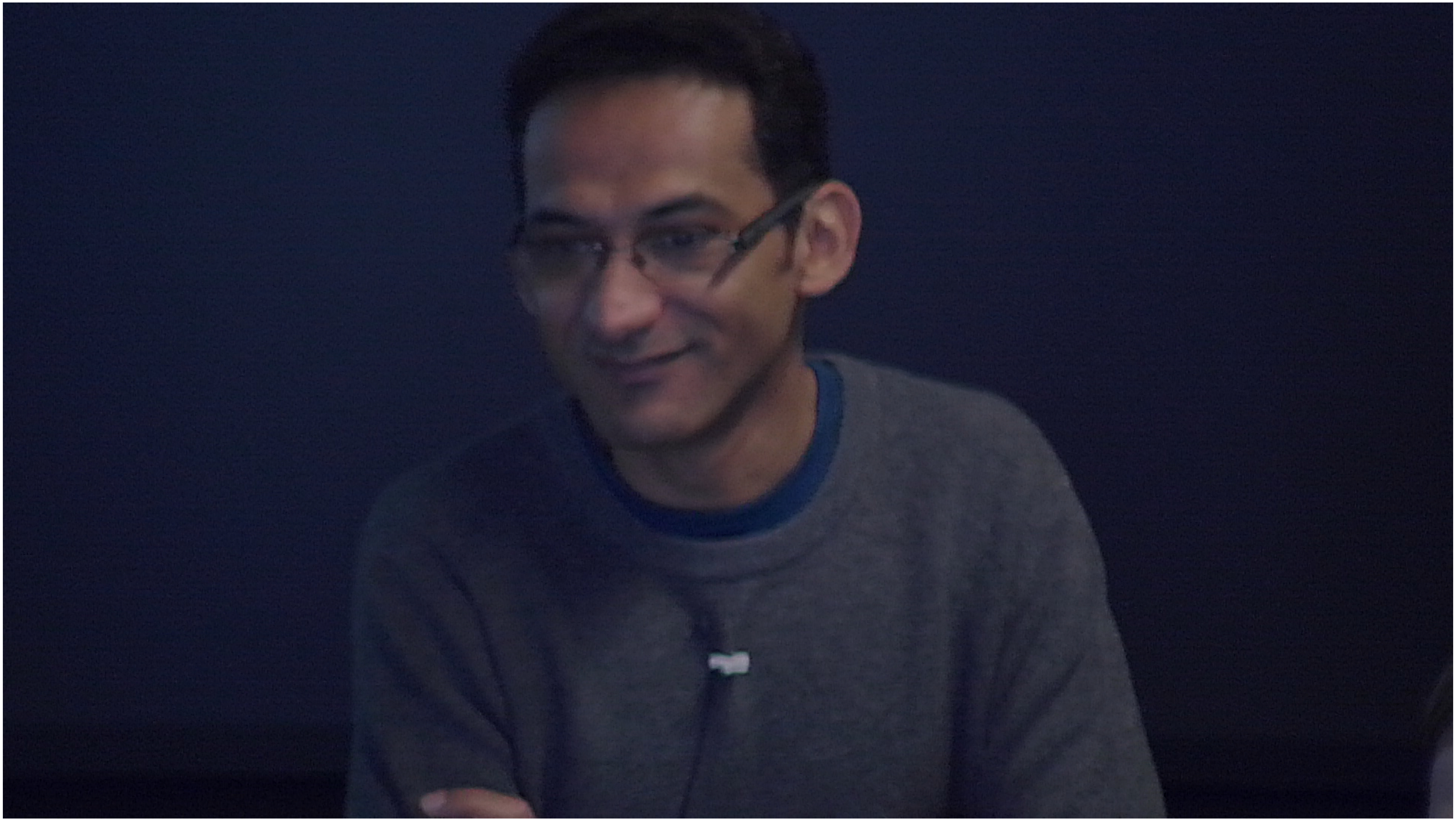

The Pierre Auger Observatory

3000 km² surface array (1660 detectors)

1.5 km triangular grid

27 fluorescence telescopes

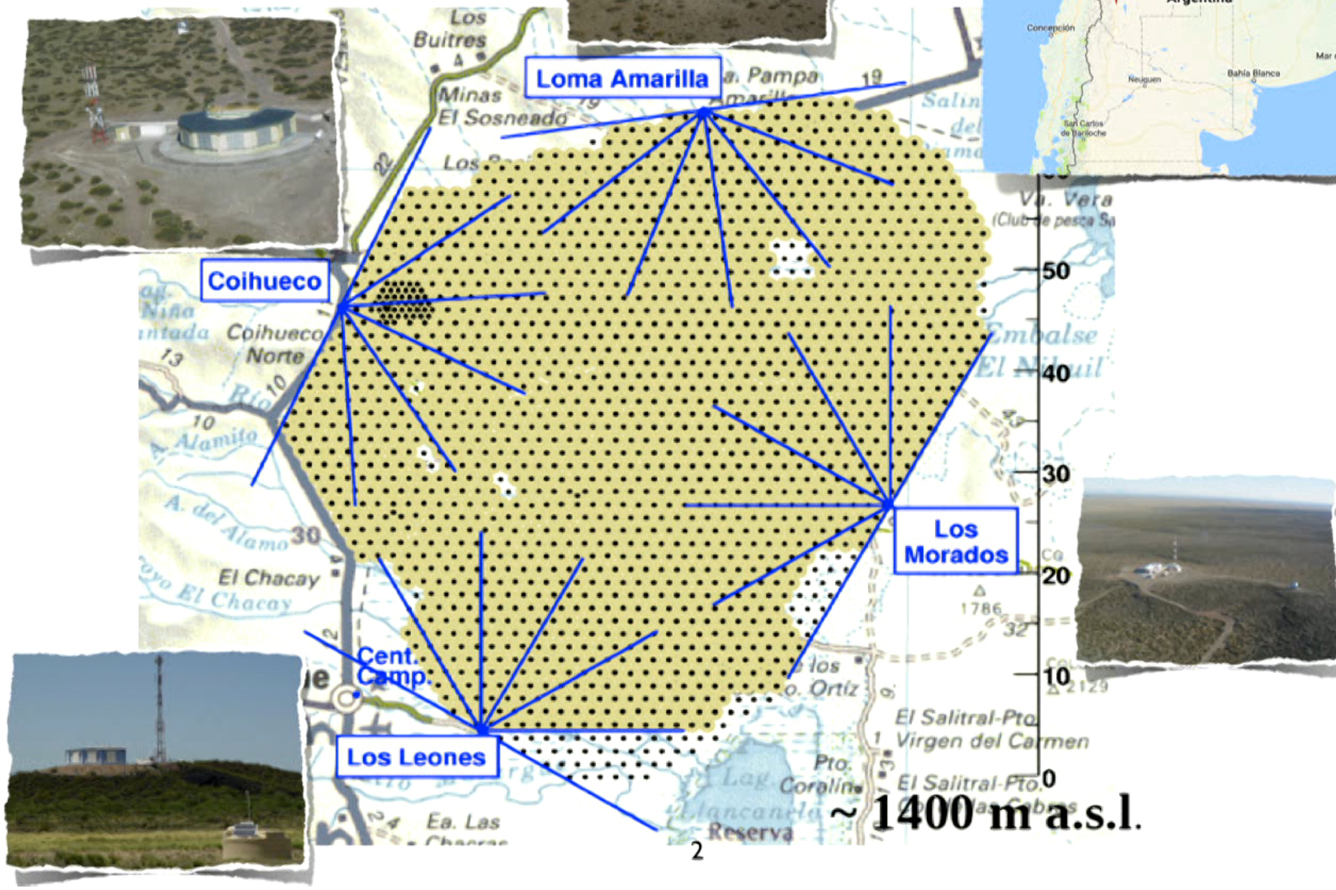

2

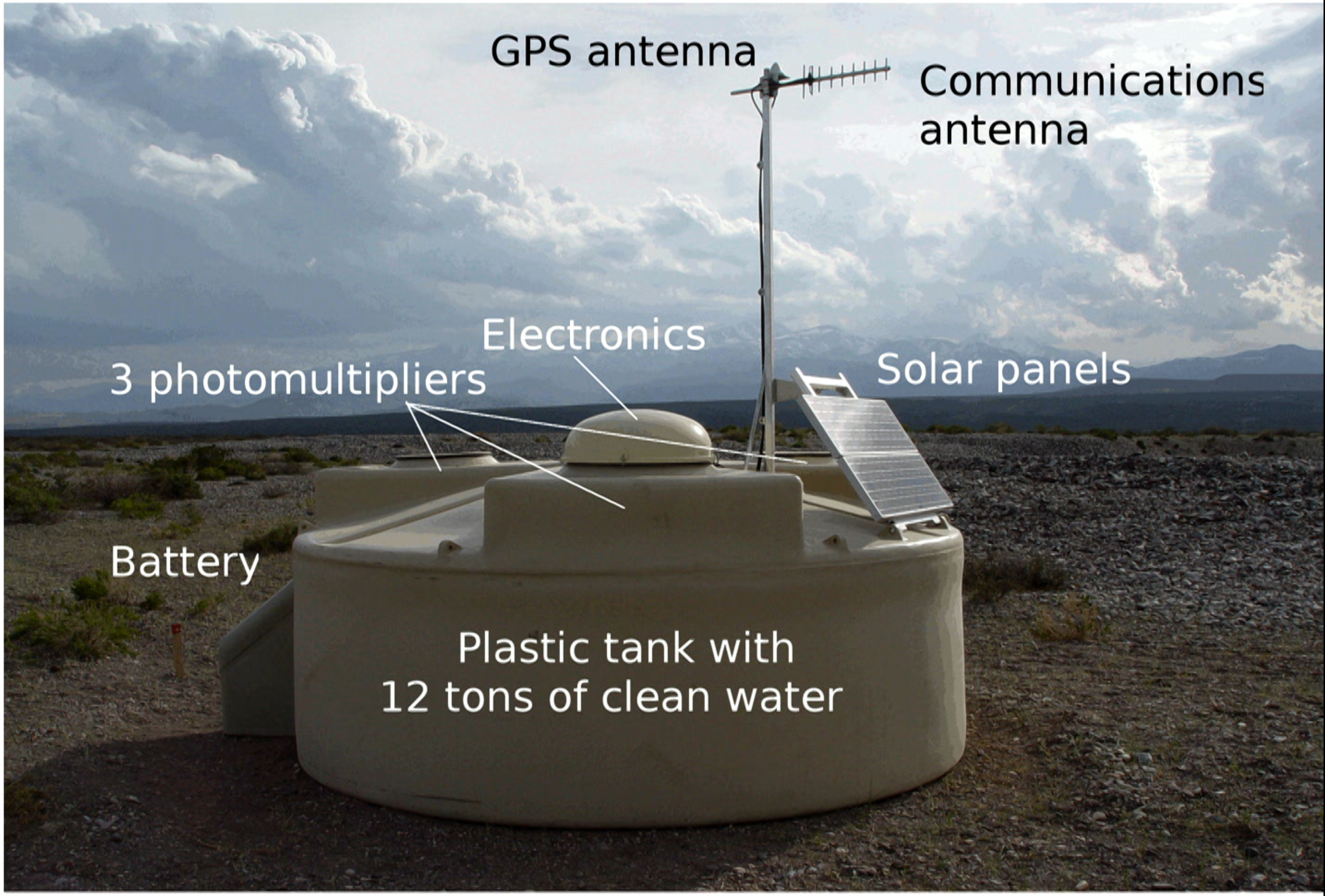
GPS antenna
Communications
antenna
Electronics
3 photomultipliers
Solar panels
Battery
Plastic tank with
12 tons of clean water

3

Surface detector vertical event reconstruction

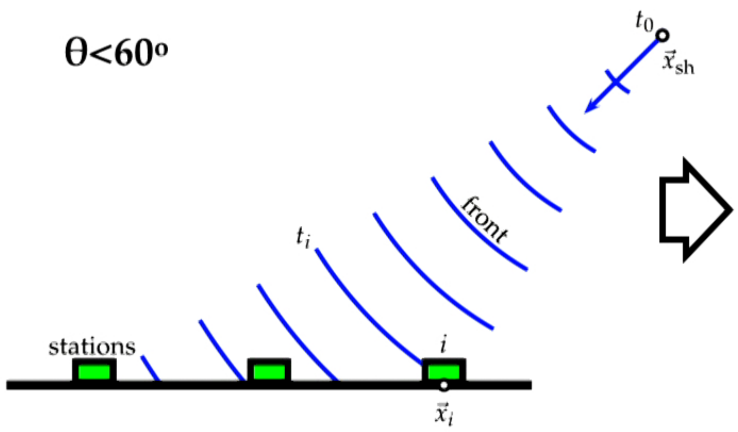

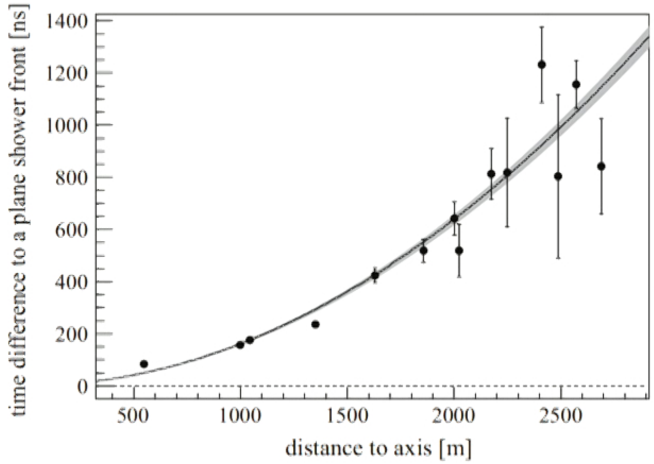

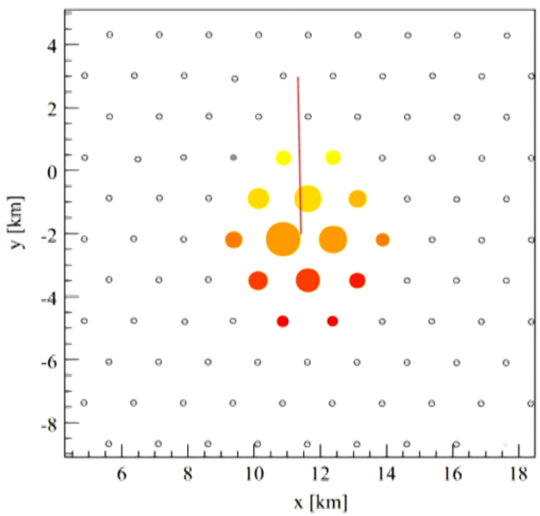

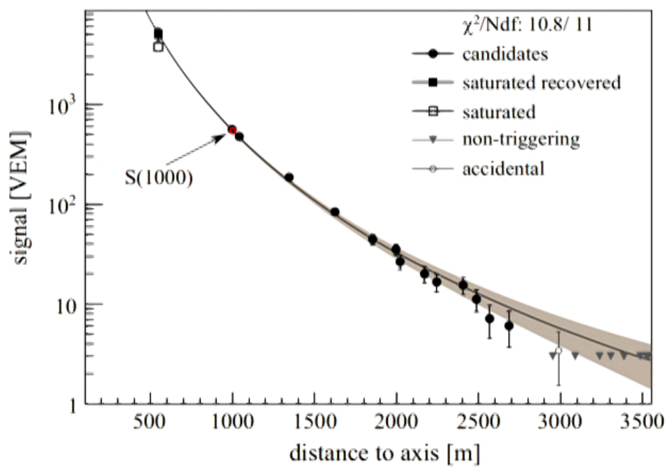

Inclined showers

- Showers developing at large zenith angle are strongly affected by atmospheric attenuation
- Signals at ground are muon rich
- Lateral distribution density of particles can no longer be described by a continuous function of the distance to shower axis

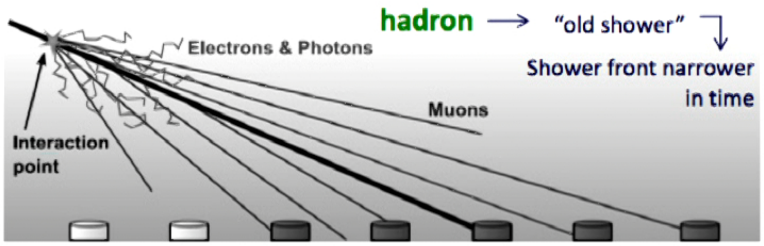

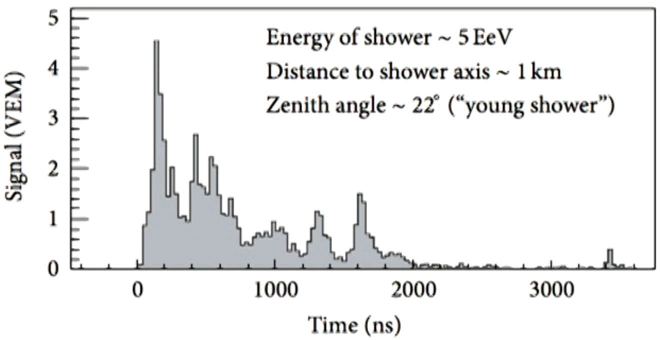

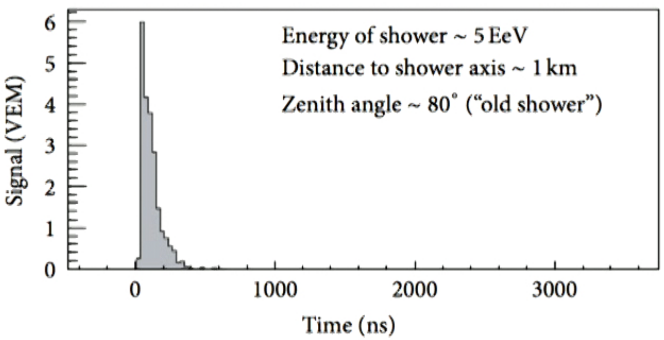

Inclined showers

- EAS muon content depends on: **energy, primary particle, zenith and azimuth**

primary, had. model, energy, geometry — **reference muon density map**

$$\rho_\mu(\vec{r}) = N_{19}\rho_{\mu,19}(\vec{r};\theta,\phi)$$

measured muon density

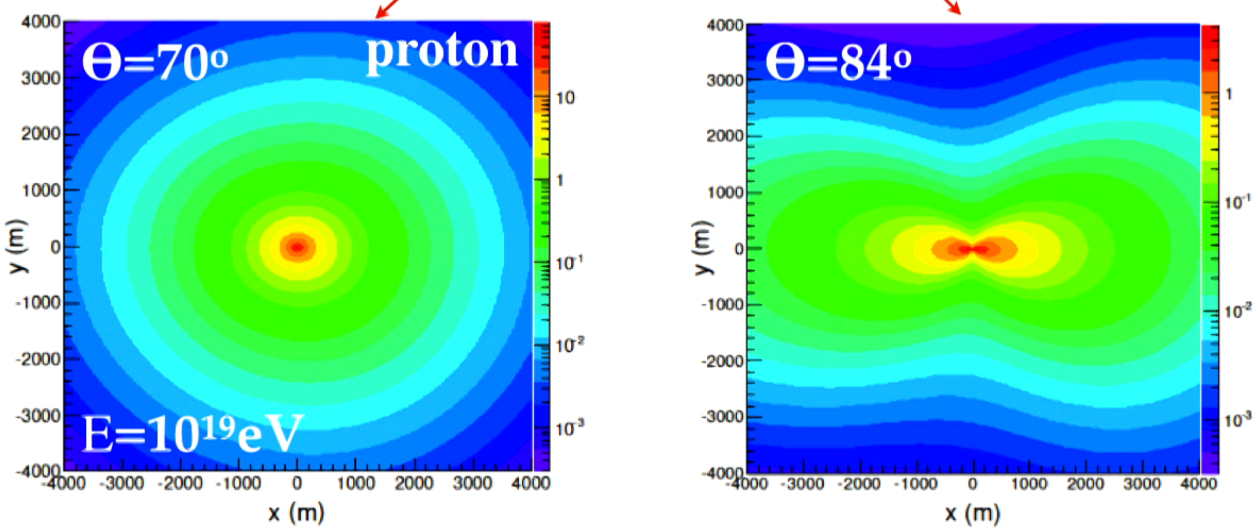

JCAP 08 (2014) 019

Hybrid event

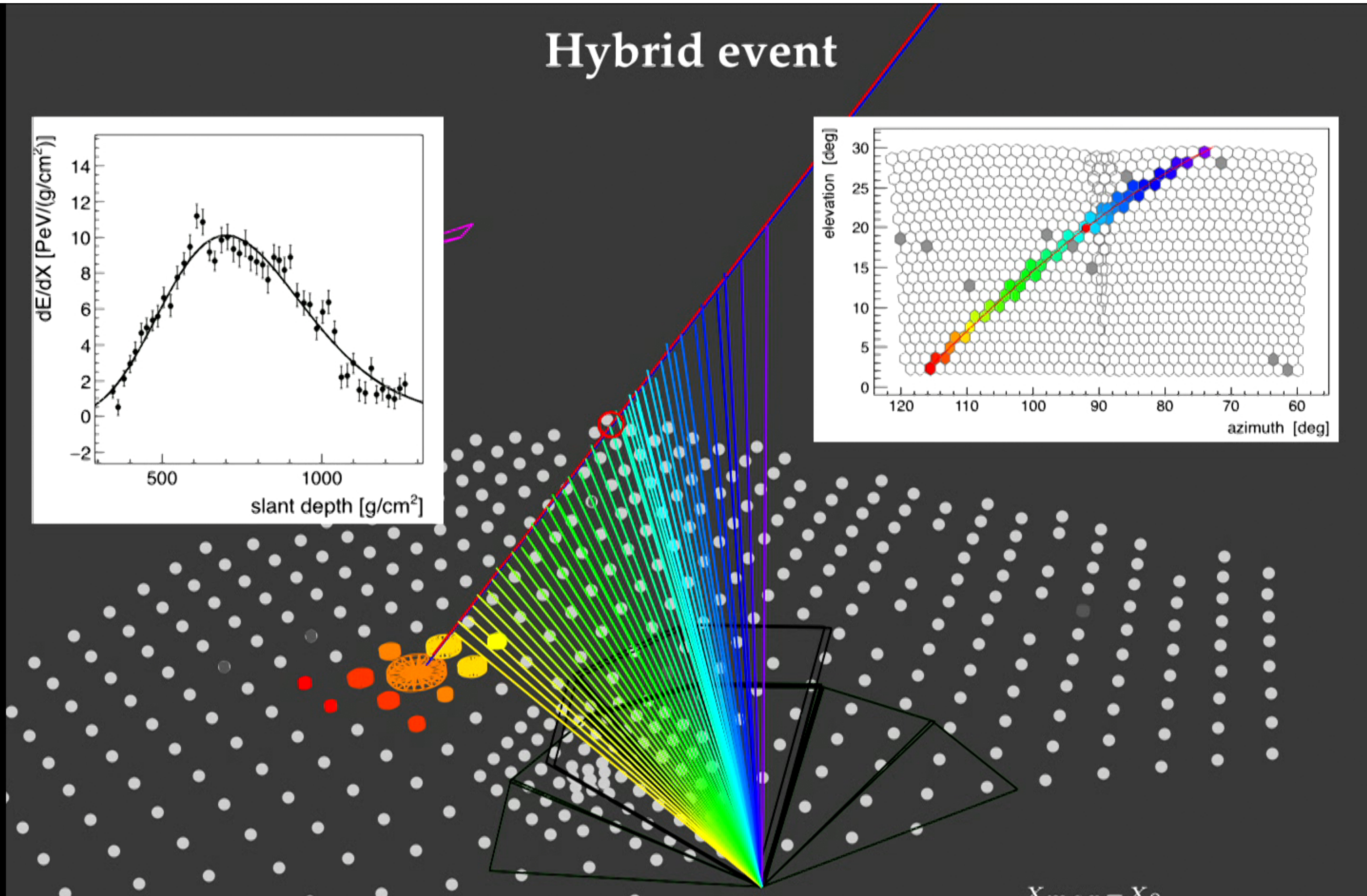

$$X = \int \rho \, dx \quad (\mathrm{g/cm^2})$$

$$N_e(X) = N_{max} \left(\frac{X - X_0}{X_{max} - X_0} \right)^{\frac{X_{max} - X_0}{\lambda}} e^{\frac{X_{max} - X_0}{\lambda}}$$

General note on Auger SD data samples - I

- Data-driven energy calibration using hybrid events
- Different SD estimators are correlated to the quasi-calorimetric energy measured by the FD
- Here, we should use two samples, depending on the zenith angle of the events:
  - Vertical: $0^o < \theta < 60^o$ (S_{38} x E_{FD})
  - Inclined: $60^o < \theta < 80^o$ (N_{19} x E_{FD})

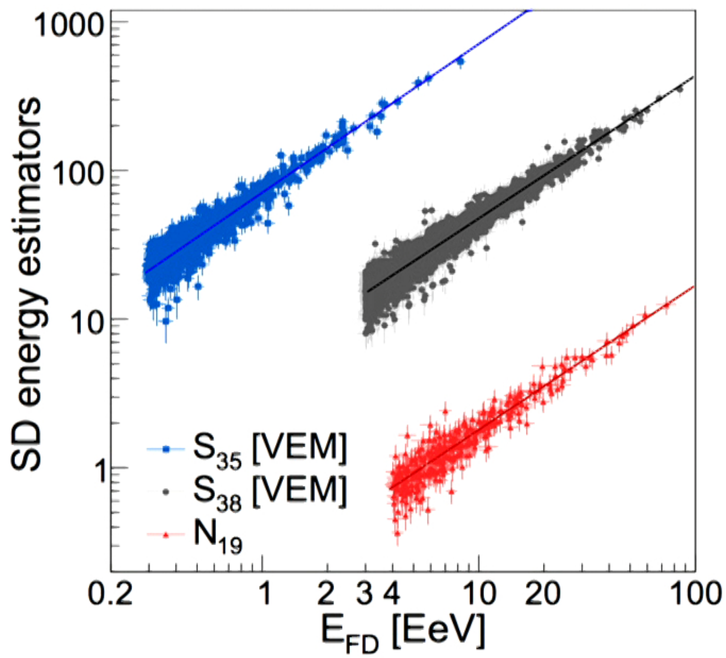

9

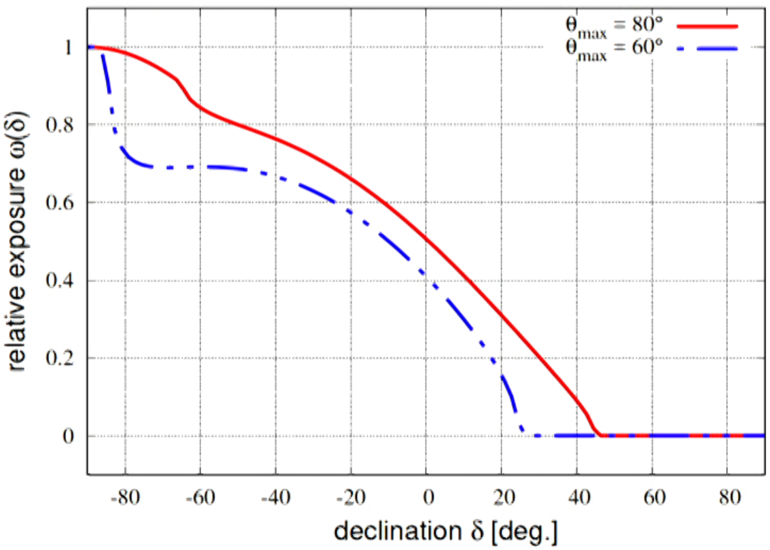

- **Inclined sample provides about ~30% of extra sky coverage**
- **This extra coverage is very important to many of the anisotropy analyses, especially the large scale ones**

vertical

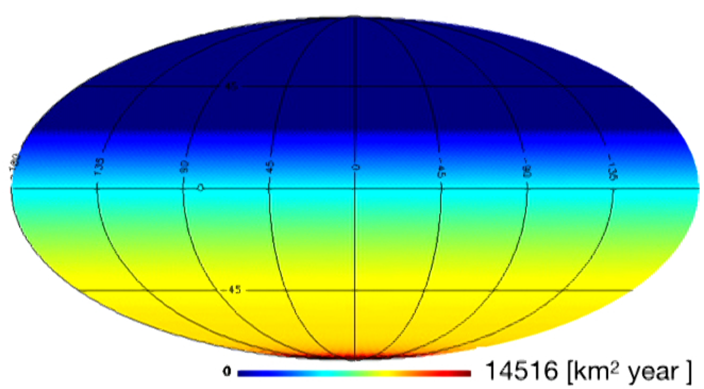

inclined

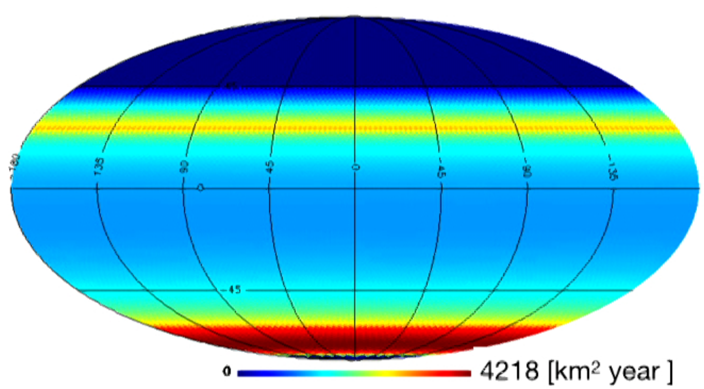

Energy spectrum

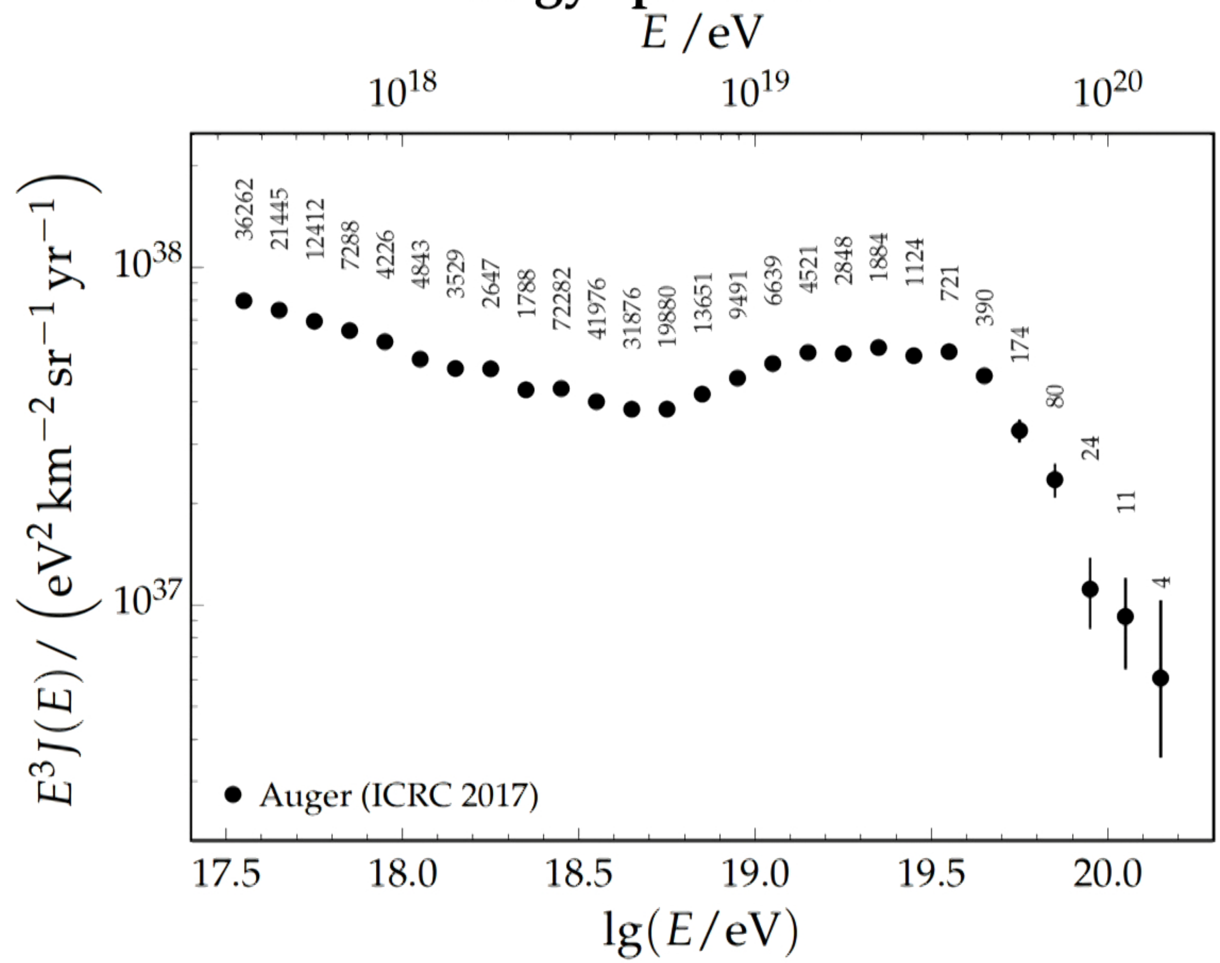

Energy spectrum

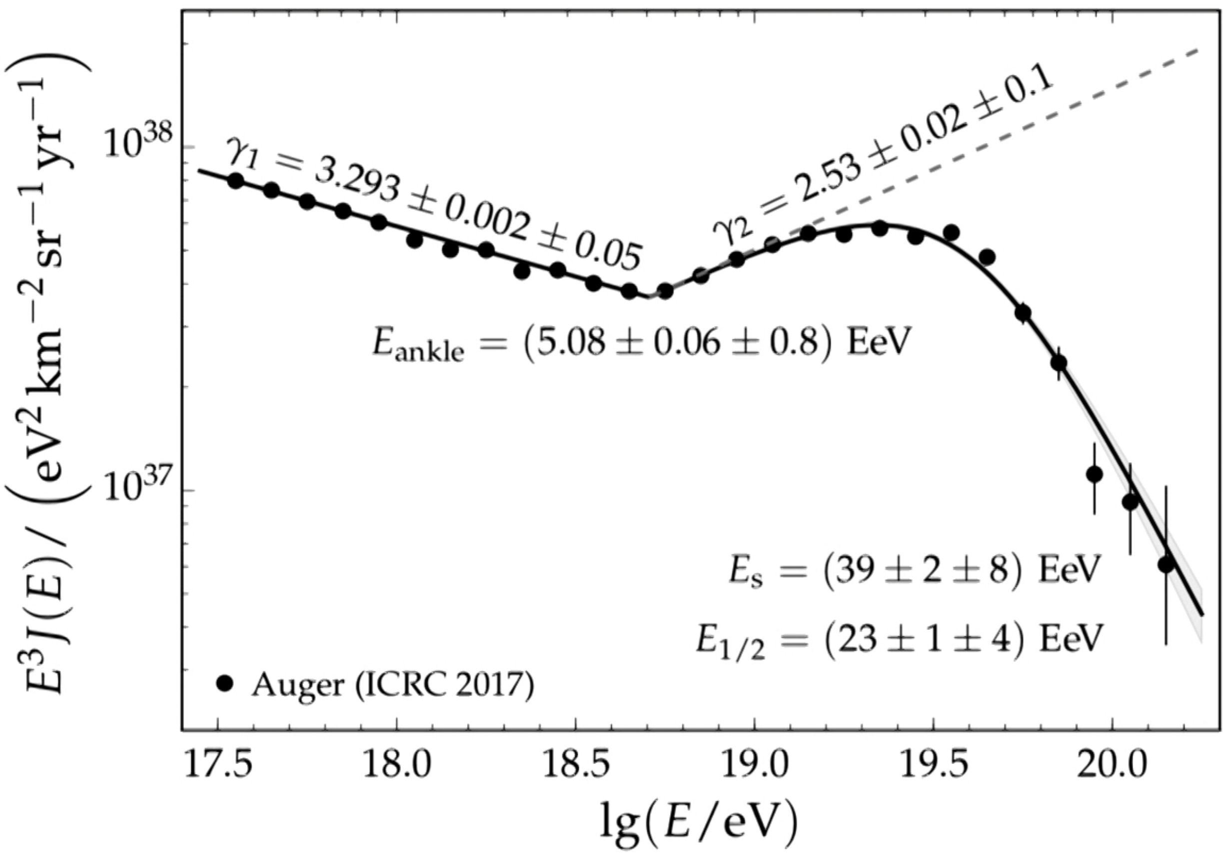

$$J_{\rm unf}(E) = \begin{cases} J_0\left(\frac{E}{E_{\rm ankle}}\right)^{-\gamma_1} & E < E_{\rm ankle} \\ J_0\left(\frac{E}{E_{\rm ankle}}\right)^{-\gamma_2}\left[1+\left(\frac{E_{\rm ankle}}{E_{\rm s}}\right)^{\Delta\gamma}\right]\left[1+\left(\frac{E}{E_{\rm s}}\right)^{\Delta\gamma}\right]^{-1} & E > E_{\rm ankle} \end{cases}$$

The GZK (Greizen-Zatsepin-Kusmin) effect

PRL 16 (17): 748

J. of Exp. and Theor. Phys. Lett. 4: 78.

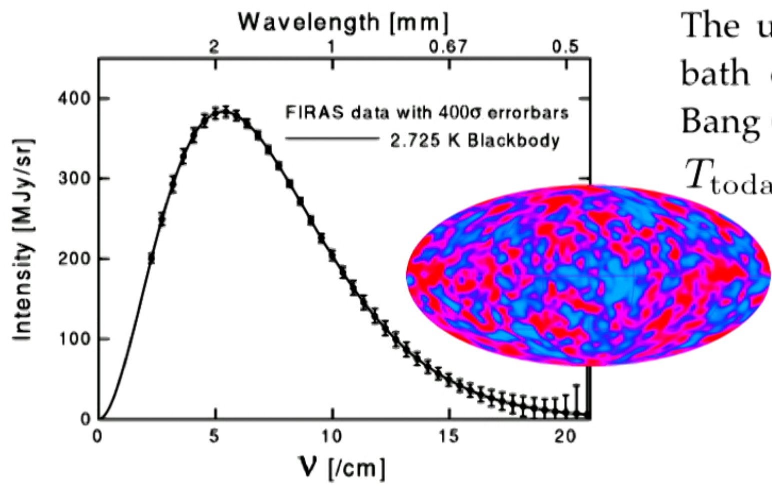

The universe is filled with an almost isotropic bath of photons produced right after the Big Bang (CMB)

$$T_{\rm today} \sim 2.75\ {\rm K} \Longrightarrow E_\gamma = k_B T \sim 10^{-4}\ {\rm eV}$$

$$\Delta^+(1232)$$

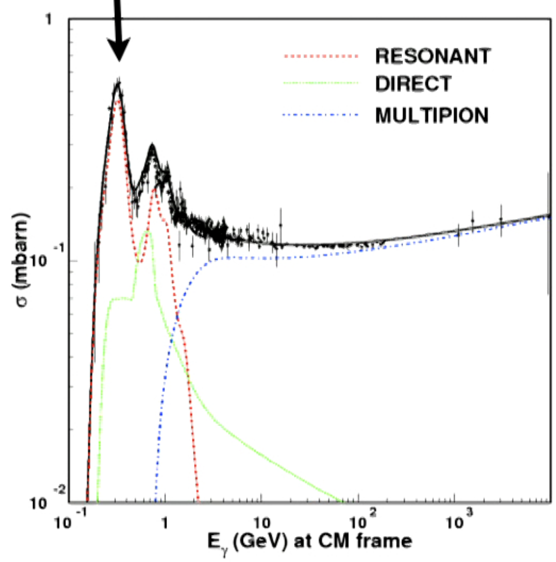

However in the frame of 5x10[19] eV proton:

$$E'_\gamma = \gamma E_\gamma \quad (\gamma \sim 10^{10})$$

$$p + \gamma_{\rm cmb} \to \Delta^+ \to p + \pi^0$$
$$p + \gamma_{\rm cmb} \to \Delta^+ \to n + \pi^+$$

$$\pi^0 \to \gamma\gamma \qquad \pi^+ \to \mu^+ + \nu_\mu$$

13

Photonuclear disintegration

@ nucleus rest-frame:

photon-nucleus cross-section at MeV energies dominated by **GDR (Giant Dipole Resonance)**

collective oscillation mode of the nucleus: protons against neutrons (induced dipole moment)

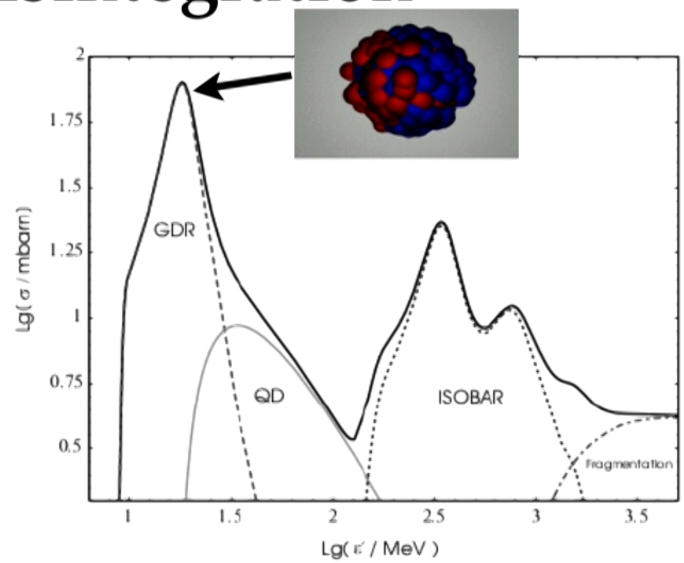

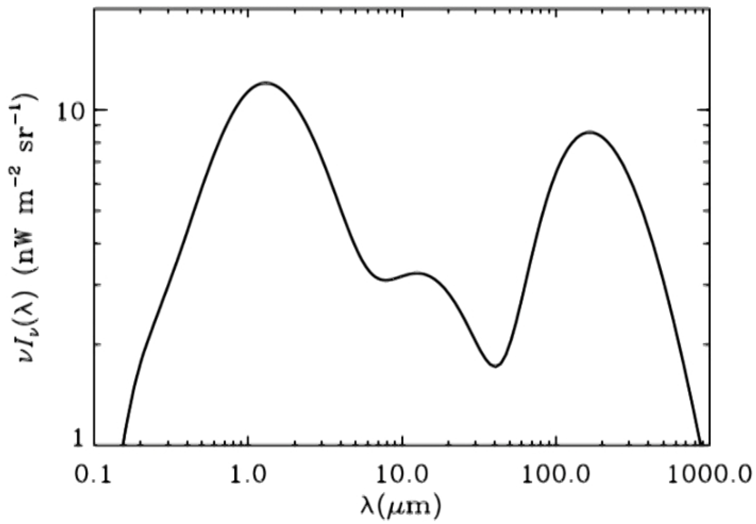

Infrared is important for nuclei

$$\epsilon_{\rm GDR} \simeq 80 A^{-1/3}\ \rm MeV$$

$$\epsilon_1/\epsilon_2 \simeq (A_1/A_2)^{2/3}$$

Usually, light nuclei disintegrate faster than heavy ones

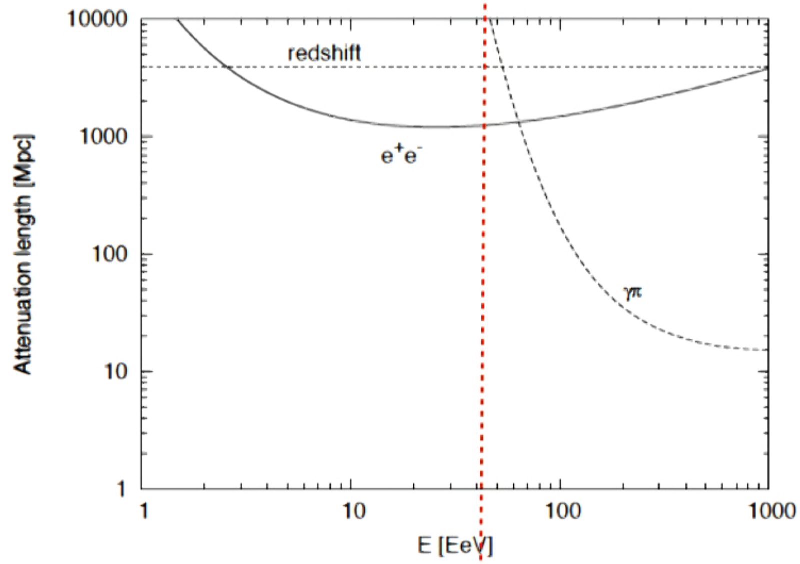

Universe should be very isotropic at "low" energies...

and become anisotropic above the GZK threshold

from Kravtsov DM simulations

The Hillas plot

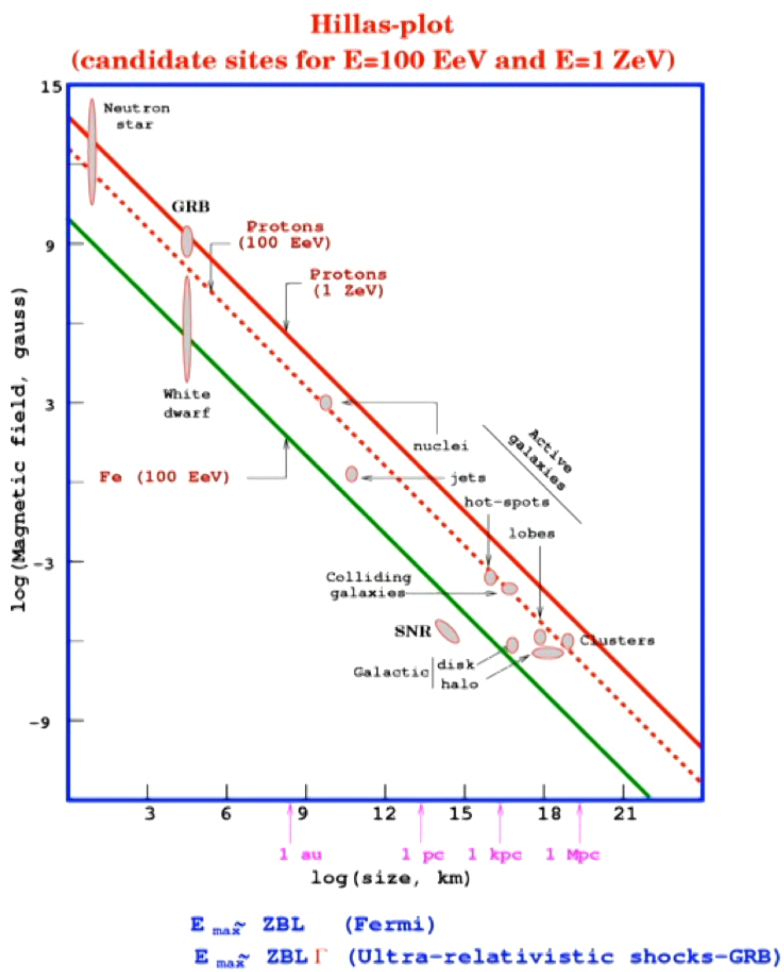

1 EeV = 10^{18} eV

1 ZeV = 10^{21} eV

➤ There should be a compromise between the source size and its magnetic field

➤ Larmor radius has to adjust to the source size

$$R_L = \frac{\gamma m v_\perp}{qB}$$

➤ Energy losses impose additional constraints to the source candidates!

16

Small to intermediate scale anisotropies

Centaurus A

1 EeV = 10^{18} eV

scan in E_{th} in 1 EeV steps

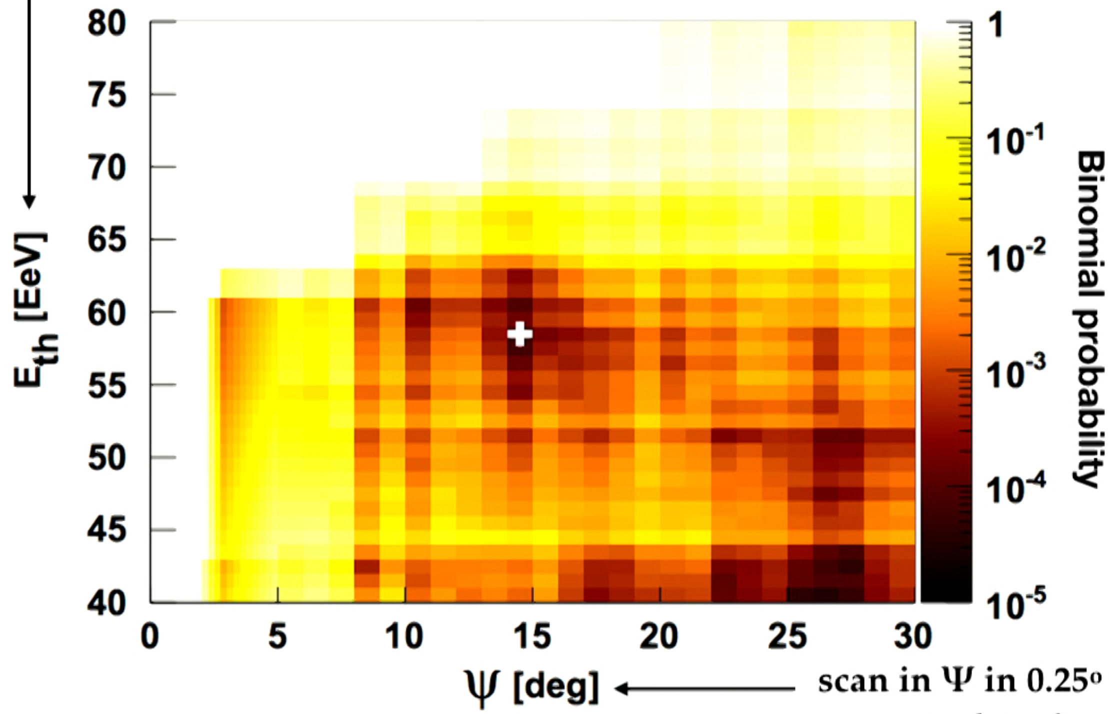

scan in Ψ in 0.25° up to 5° and 1° above

Minimum probability found at:

$E_{th} = 58$ EeV, $\Psi = 15°$

$n_{obs} = 19$, $n_{exp} = 6.0$

$P \sim 1.1 \times 10^{-5}$

Post-trial (E_{th}, Ψ):

$\sim 1.1 \times 10^{-3}$

Selection of extragalactic gamma-ray sources

- AGNs and starburst galaxies seem to dominate the x-gal γ-ray background

Di Mauro & Donato, PRD 91 (2015) 123001

EGB composition with MW SF model

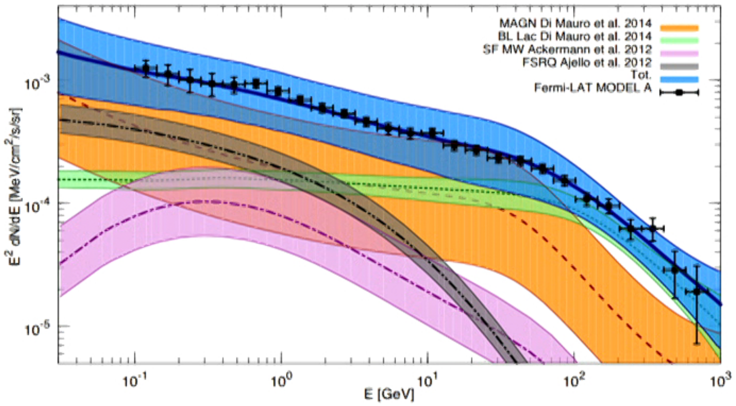

- Assuming that the UHECR flux is correlated to the non-thermal photon flux:

Starburst galaxies

- Fermi-LAT list of star-formation objects (Ackermann+12)
- $\Phi(>1.54\text{ GHz})$ as proxy for UHECR flux
- Brightest objects selected: $\Phi(>1.54\text{ GHz}) > 0.3$ Jy
- 23 objects in final sample

Active Galactic Nuclei

- Fermi 2FHL catalog
- $\Phi(>50\text{ GeV})$ as proxy for UHECR flux
- 17 objects up to 250 Mpc
- Most blazars and BL-Lac type

Construction of the likelihood

Un-binned likelihood:

exposure → $\omega(\hat{\mathbf{n}}_i)$

$$\mathscr{L} = \prod_{i=1}^{N} [\omega(\hat{\mathbf{n}}_i) \times \mathrm{model}(\hat{\mathbf{n}}_i)]$$

model:

$$[\alpha \times \mathrm{sources} + (1-\alpha) \times \mathrm{isotropy}] \otimes \mathrm{Gaussian}(\theta)$$

Include weights to account for flux attenuation (especially important for AGNs)

2D parameter space (α,θ):
- **α: Anisotropic fraction**
- **θ: RMS deflection**

Scan in energy threshold [20:80] EeV in steps of 1 EeV

Test statistics (TS) is a log-likelihood ratio of two hypotheses:

$$\mathrm{TS} = 2\ln\left(\frac{H_1}{H_0}\right)$$

- H_1: **AGN or starburst as sources**
- H_0: **Isotropy**

TS vs threshold energy

ICRC2017

Starburst Galaxies
TS = 24.9, E_{th} = 39 EeV

γ-ray detected AGNs
TS = 15.2, E_{th} = 60 EeV

***Swift*-BAT AGNs**
TS = 19.9, E_{th} = 60 EeV

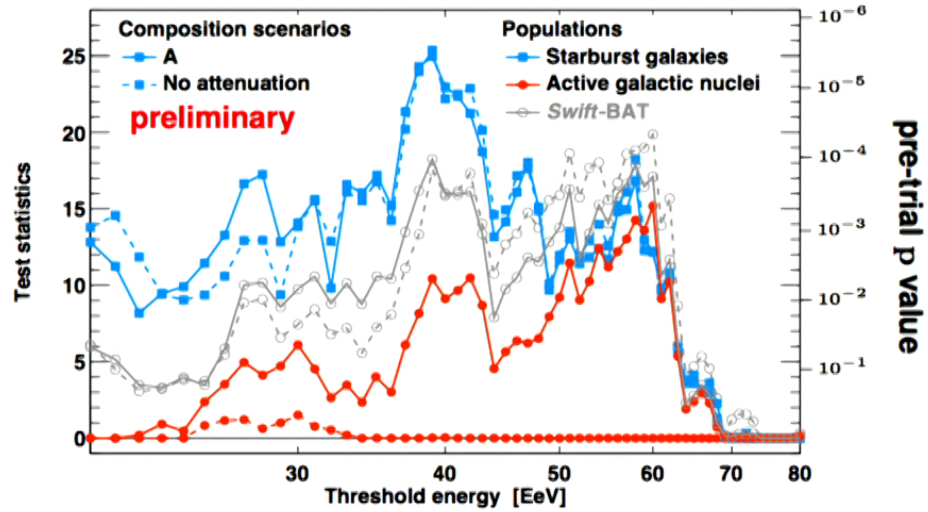

- Flux attenuation weights very important for AGNs, but negligible for starburst (nearby)
- Weights, however, depend strongly on the mass composition scenario

Mass composition scenario:
- Combined spectrum+Xmax fit
- EPOS-LHC as hadronic model
- Uniform source distribution

Element	Fraction
H	0%
He	67.3%
N	28.1%
Si	4.6%
Fe	0%

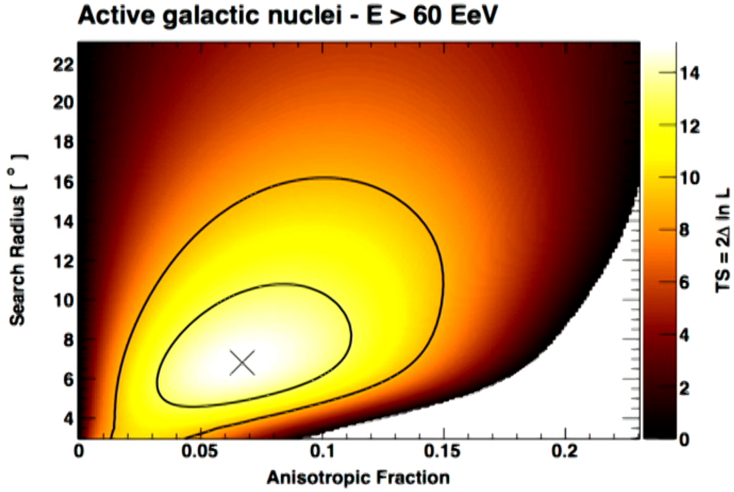

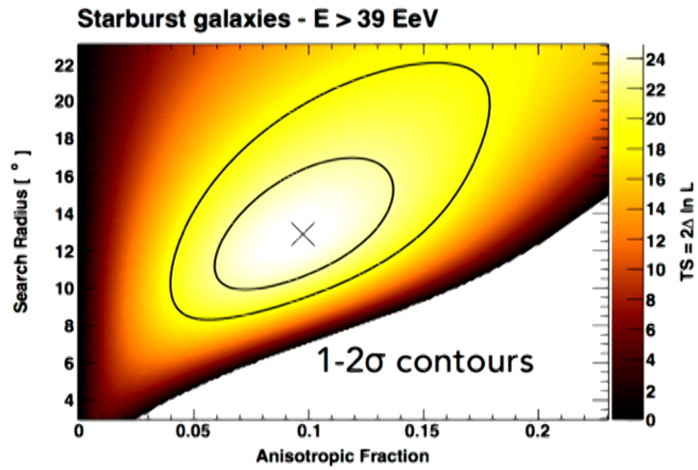

$$\alpha = 7\%,\ \theta = 7^\circ$$

TS = 15.2

E_{th} = 60 EeV

Pre-trial: 5 x 10^{-4}

Post-trial: 3 x 10^{-3} (2.7σ)

$$\alpha = 10\%,\ \theta = 13^\circ$$

TS = 24.9

E_{th} = 39 EeV

Pre-trial: 4 x 10^{-6}

Post-trial: 4 x 10^{-5} (3.9σ)

- **Post-trial prob. = fraction of isotropic simulations with TS greater than in data while scanning across the same energy bins**
- **Previous searches and hidden trials not account for**

Best-fit maps (galactic coord.)

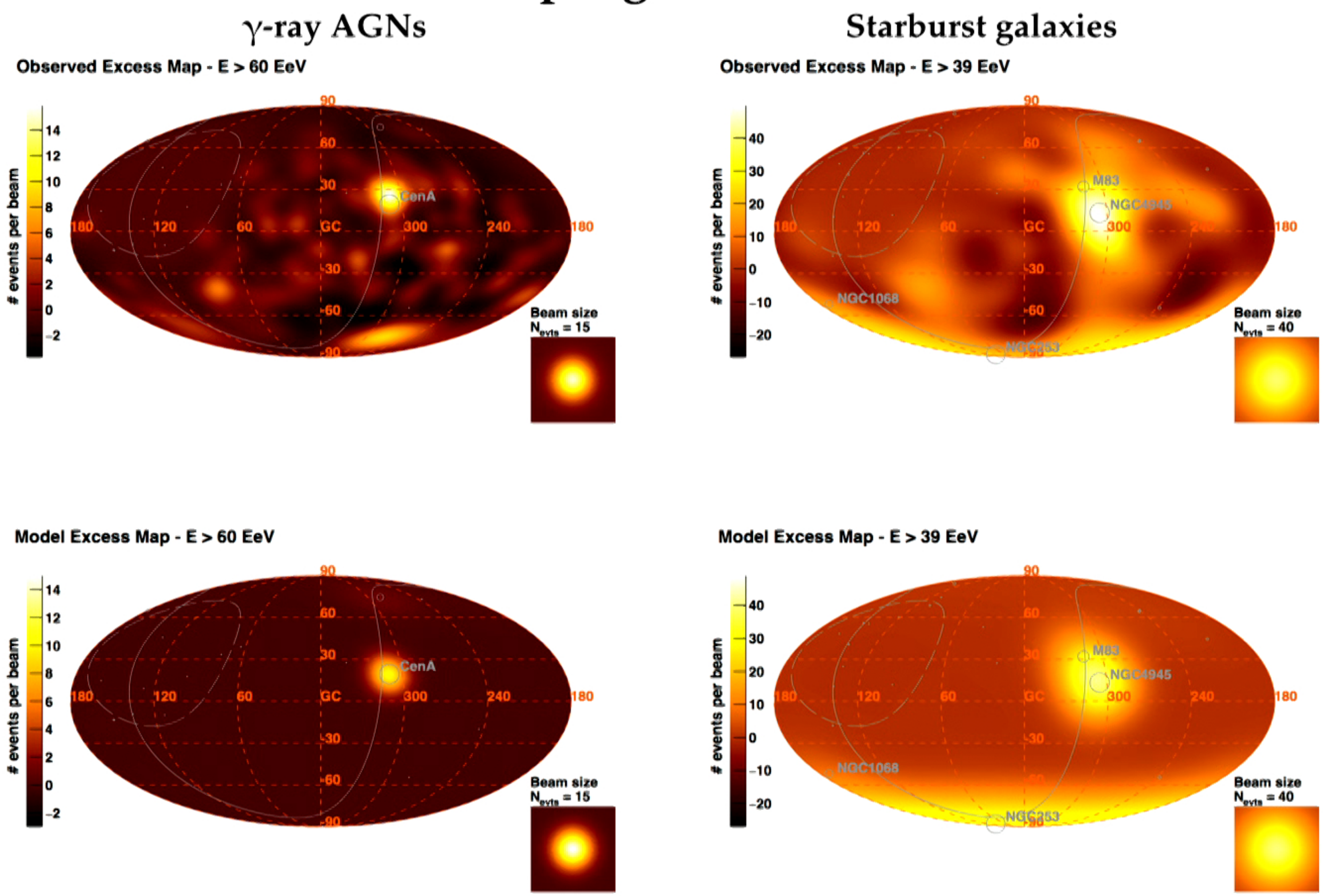

23

Large scale anisotropies

Previous upper limits

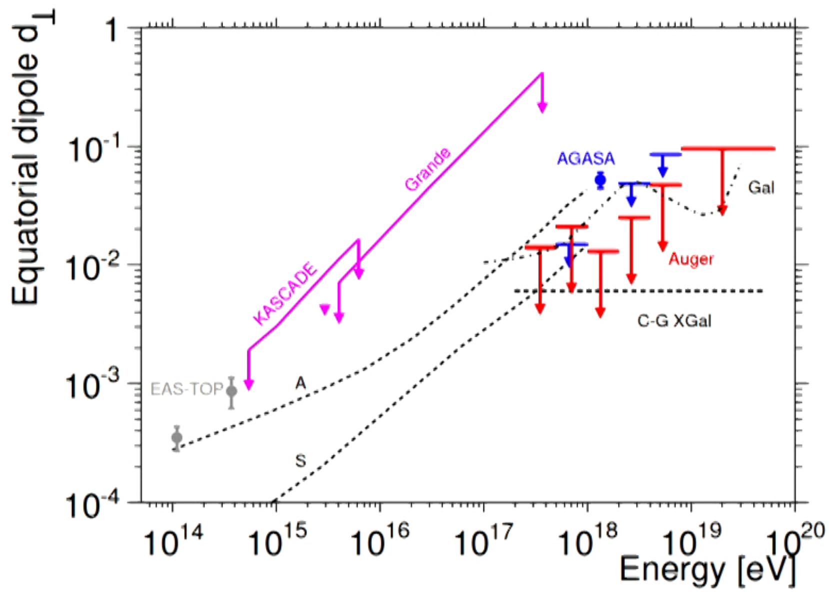

Weather modulation of the trigger rate

- Pressure and density are the main variables attached to the cascade development
- In a first approximation, pressure defines the "age" of the shower when it reaches the ground
- Density affects the lateral distribution of particles by determining the Molière radius of the shower
- The modulation is a threshold effect, because the shower size is coupled to the atmospheric variables
- Modeling the rate enables us to correct the signal at shower-to-shower basis

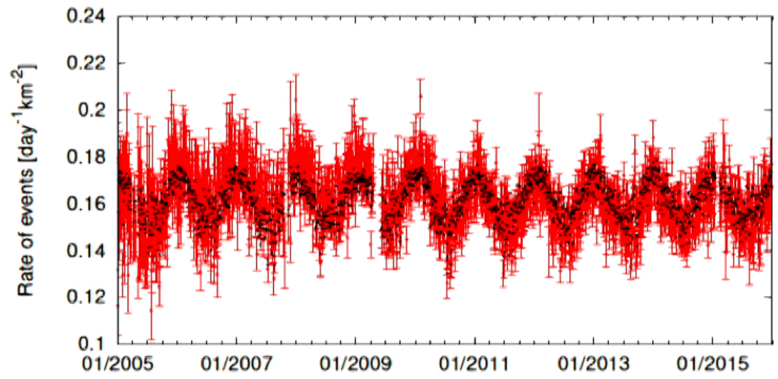

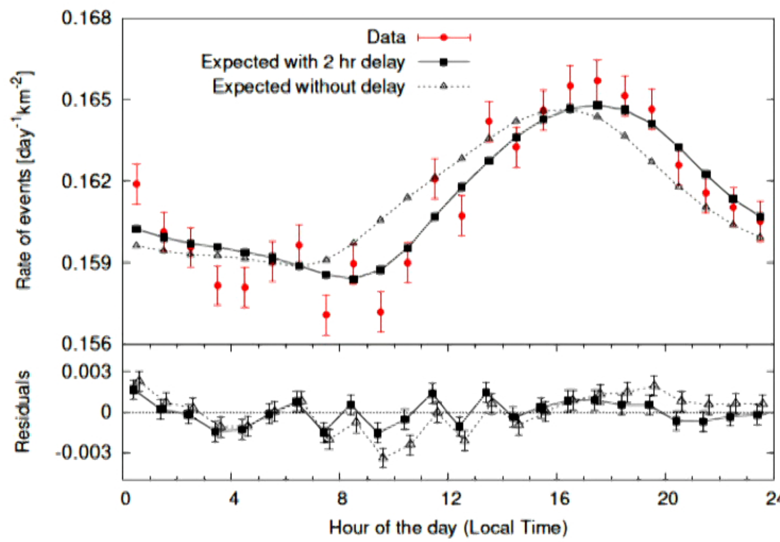

JINST 12 P02006 (2017)

Why should we care about weather modulations?

- **Fast daily variations modulated by slow annual ones can be seen as the interference between two frequencies: sidereal and anti-sidereal**

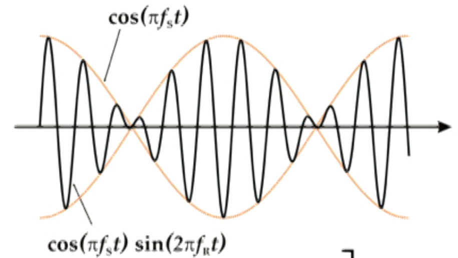

$$\underbrace{A_1 \cos\left(2\pi \frac{f_1 + f_2}{2} t\right)}_{\text{solar}} \times \underbrace{A_2 \cos\left(2\pi \frac{f_1 - f_2}{2} t\right)}_{\text{diurnal}} = \frac{A_1 A_2}{2} \left[\underbrace{\cos(2\pi f_1 t)}_{\text{sidereal}} + \underbrace{\cos(2\pi f_2 t)}_{\text{anti-sidereal}}\right]$$

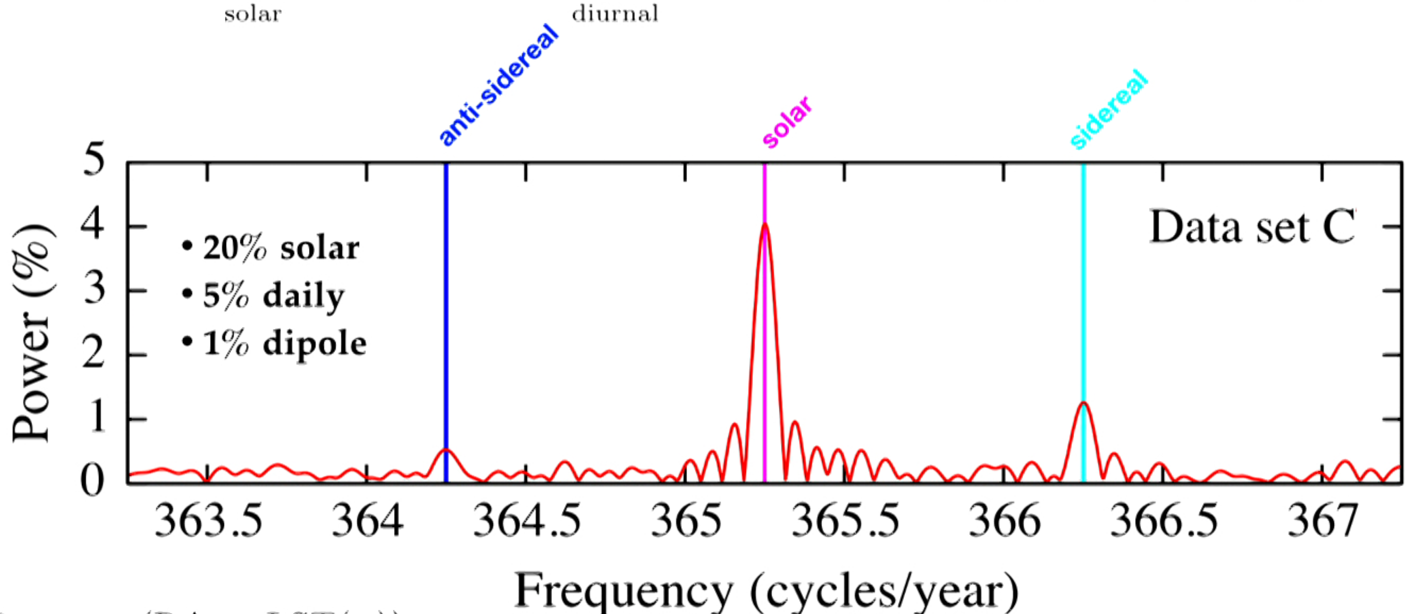

$\xi_i = t_i + (\mathrm{RA}_i - \mathrm{LST}(t_i))$

Astropart. Phys. 29, 1 (2008) 14

27

Geomagnetic correction

JCAP11 (2011) 022

- Geomagnetic field distorts the muon distribution at ground level
- The magnitude of the effect will depend on the transverse component of the field for a given shower geometry

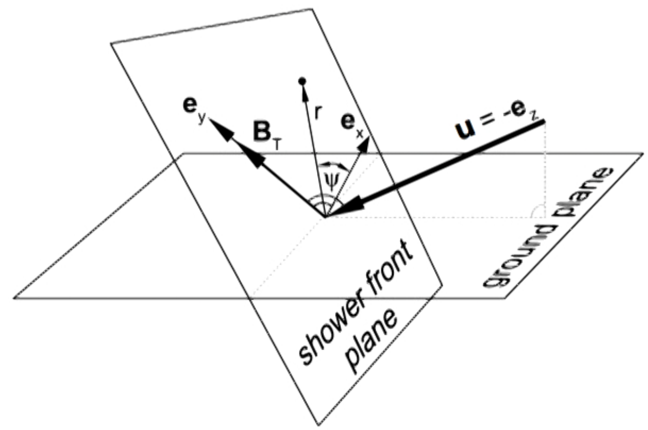

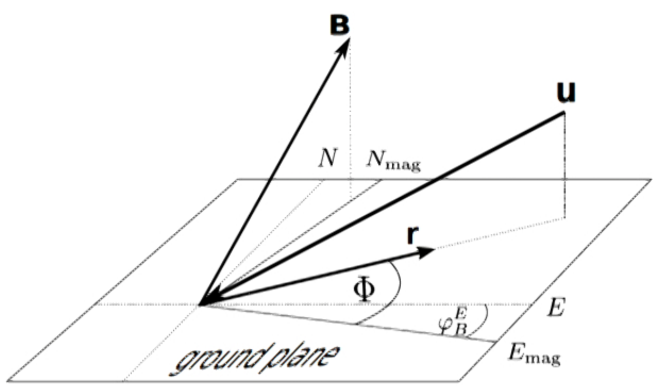

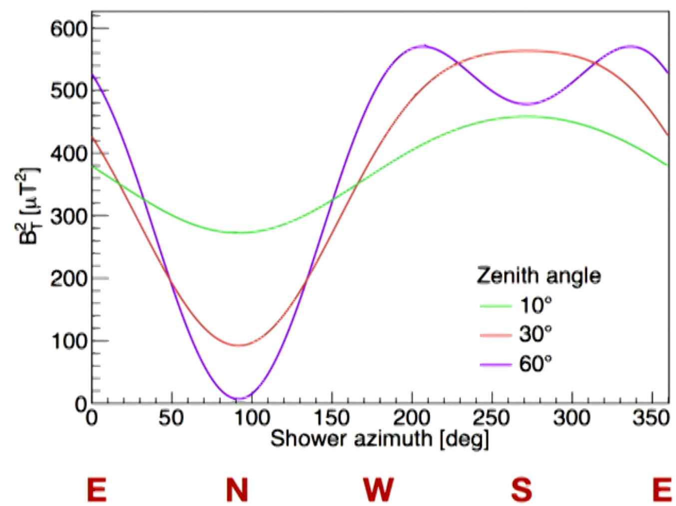

Geomagnetic correction

JCAP11 (2011) 022

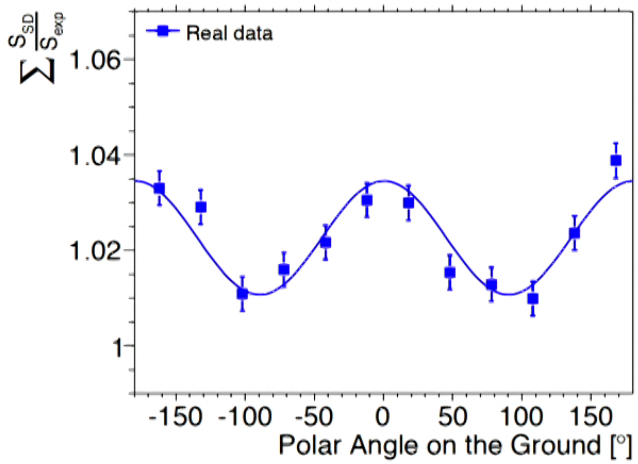

- At the station level, the signal modulation at ground is nicely reproduced by simulations
- At the shower level, modulation of S(1000) is also well understood
- Amplitude of the effect, rises fast with zenith angle above 50º

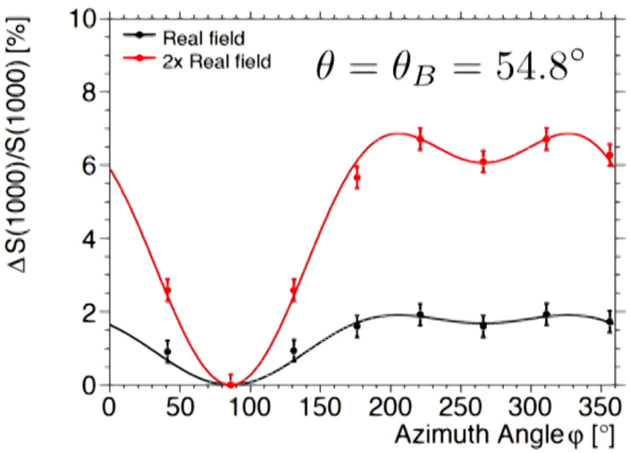

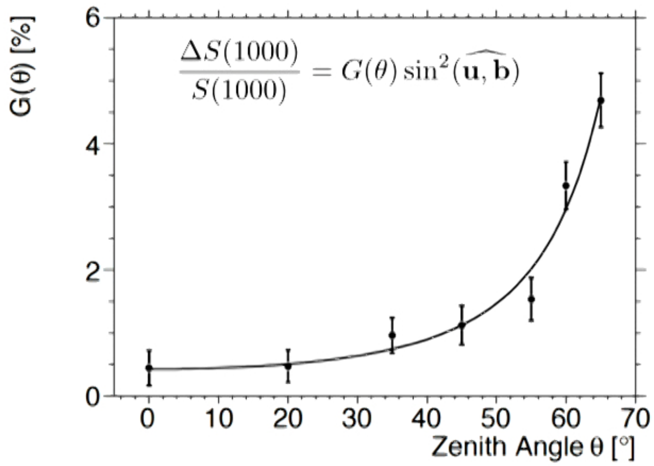

Why should we care about geomagnetic field?

JCAP11 (2011) 022

- Shower size bias is zenith angle dependent
- After averaging over azimuth and time, part of this bias leaks into the declination distribution
- Bias introduces a fake ~2% dipolar pattern on the sky along directions close to South Pole

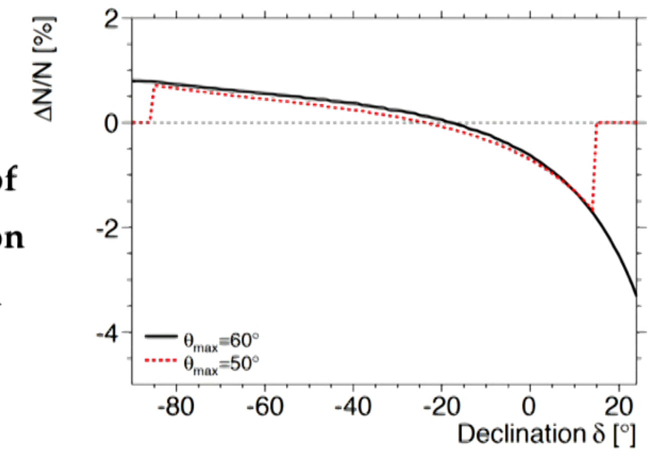

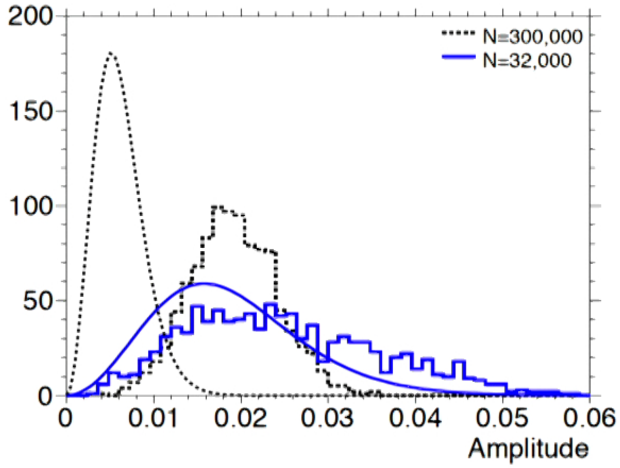

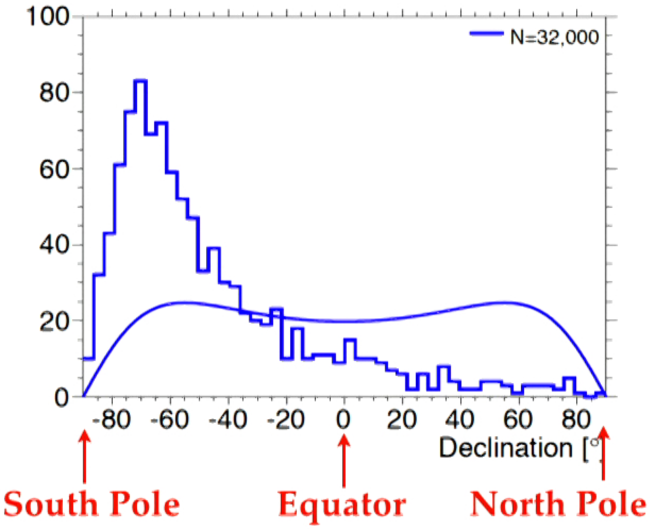

30

Sidereal time modulation of the exposure

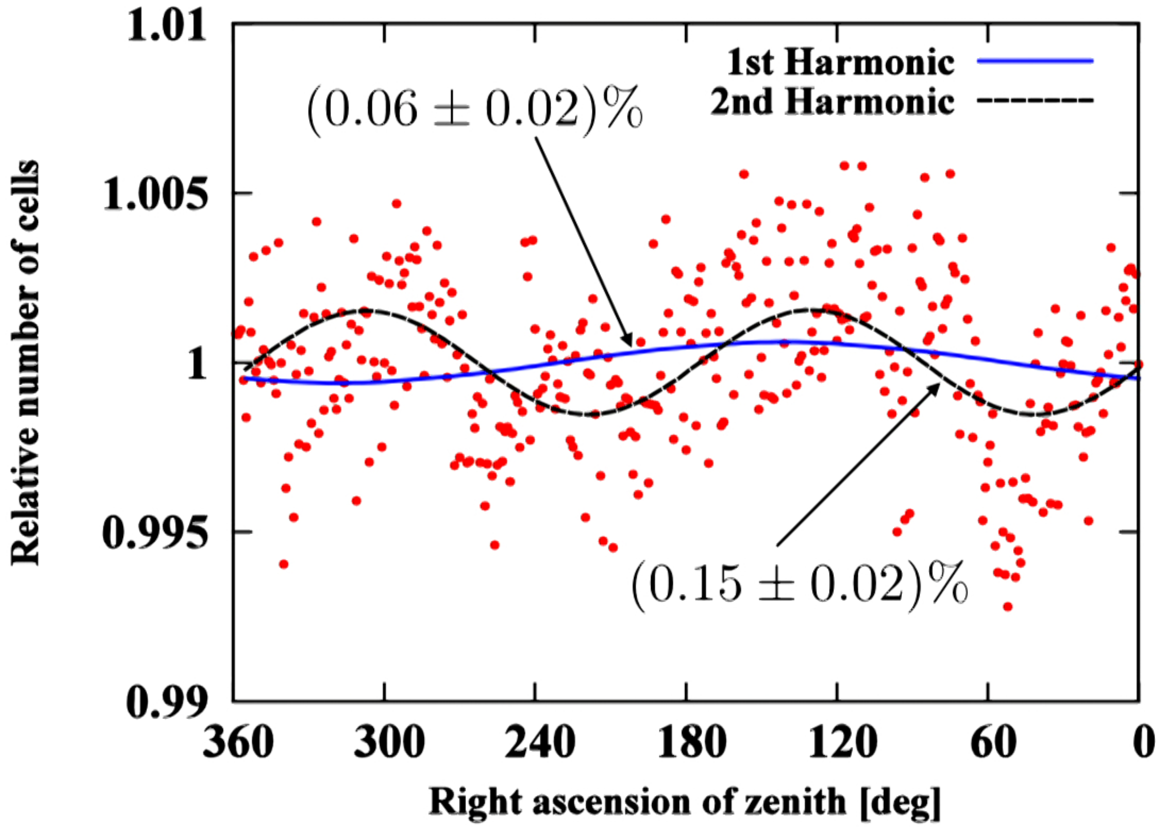

Dipole above 8 EeV (8×10^{18} eV) - dataset

- Period: 01-01-2004 to 08-31-2016
- Additional sky coverage (~30%) provided by inclined events ($60^o<\theta<80^o$)
- Enhanced statistics (~19%) with the use of relaxed (but high quality) triggers
- Total integrated exposure of 76,800 km^2 sr year

Directional exposure

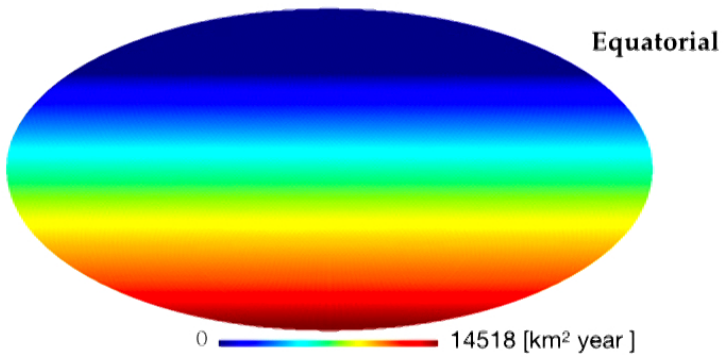

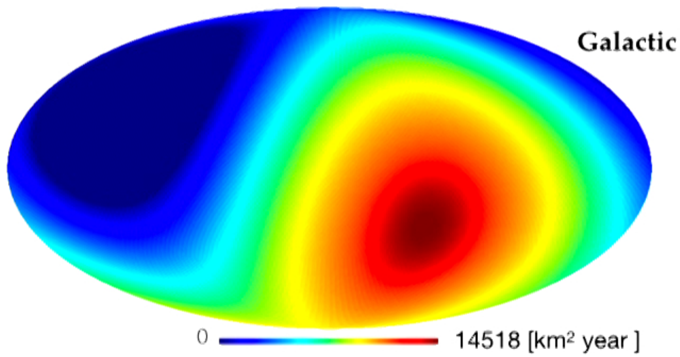

Dipole detection

Science 57 (2017) 1266

Analysis of first harmonic modulation in RA and azimuth

$$a_\alpha = \frac{2}{N}\sum_{i=1}^{N} w_i \cos \alpha_i$$

Account for non-uniformities of the exposure in RA and a slight tilt of the array

$$b_\alpha = \frac{2}{N}\sum_{i=1}^{N} w_i \sin \alpha_i$$

Amplitude and phase of modulation

$$r_\alpha = \sqrt{a_\alpha^2 + b_\alpha^2} \qquad \tan \varphi_\alpha = \frac{b_\alpha}{a_\alpha}$$

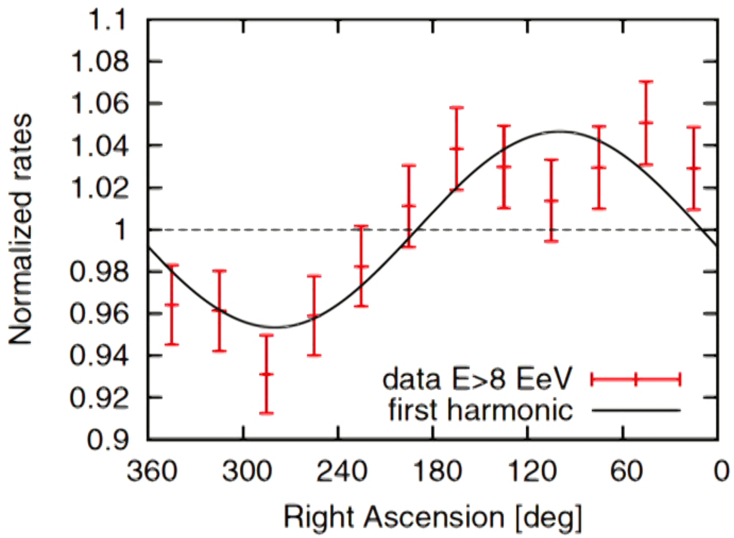

Energy (EeV)	Number of events	Fourier coefficient a_α	Fourier coefficient b_α	Amplitude r_α	Phase φ_α (°)	Probability $P(\geq r_\alpha)$
4 to 8	81,701	0.001 ± 0.005	0.005 ± 0.005	$0.005^{+0.006}_{-0.002}$	80 ± 60	0.60
≥8	32,187	−0.008 ± 0.008	0.046 ± 0.008	$0.047^{+0.008}_{-0.007}$	100 ± 10	2.6×10^{-8}

- 5.6 σ pre-trial signal
- 5.2 σ post-trial (penalized for scan in 2 energy bins)

pre-trial probability:

$$P(\geq r_\alpha) = \exp\left(-\frac{N r_\alpha^2}{4}\right)$$

Reconstruction of the 3D dipole

Science 57 (2017) 1266

Components parallel and perpendicular to the Earth rotation axis:

$$d_z \approx \frac{b_\varphi}{\cos\,\ell_{\rm obs}\langle\sin\theta\rangle} \qquad d_\perp \approx \frac{r_\alpha}{\langle\cos\delta\rangle}$$

Right ascension and declination:

$$\alpha_{\rm d} = \varphi_\alpha \qquad \tan\delta_{\rm d} = \frac{d_z}{d_\perp}$$

E>8 EeV

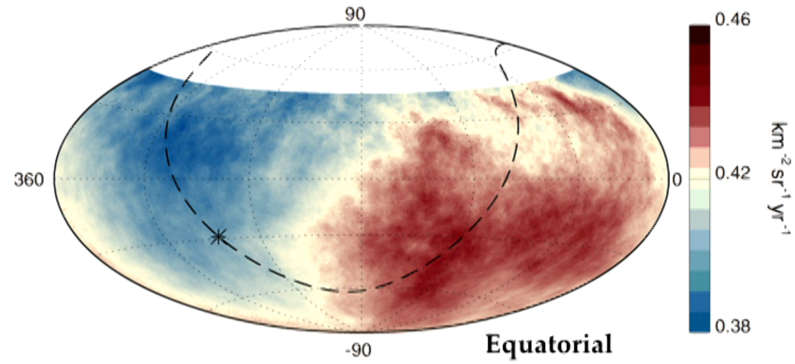

Equatorial

Energy (EeV)	Dipole component d_z	Dipole component $d_\perp$	Dipole amplitude d	Dipole declination δ_d (°)	Dipole right ascension α_d (°)
4 to 8	−0.024 ± 0.009	$0.006^{+0.007}_{-0.003}$	$0.025^{+0.010}_{-0.007}$	-75^{+17}_{-8}	80 ± 60
≥8	−0.026 ± 0.015	$0.060^{+0.011}_{-0.010}$	$0.065^{+0.013}_{-0.009}$	-24^{+12}_{-13}	100 ± 10

- **Reconstruction assumes the dipole is the dominant component of the anisotropy**
- **Analysis of the power spectrum gives support to this hypothesis**

Final sky map: galactic coordinates

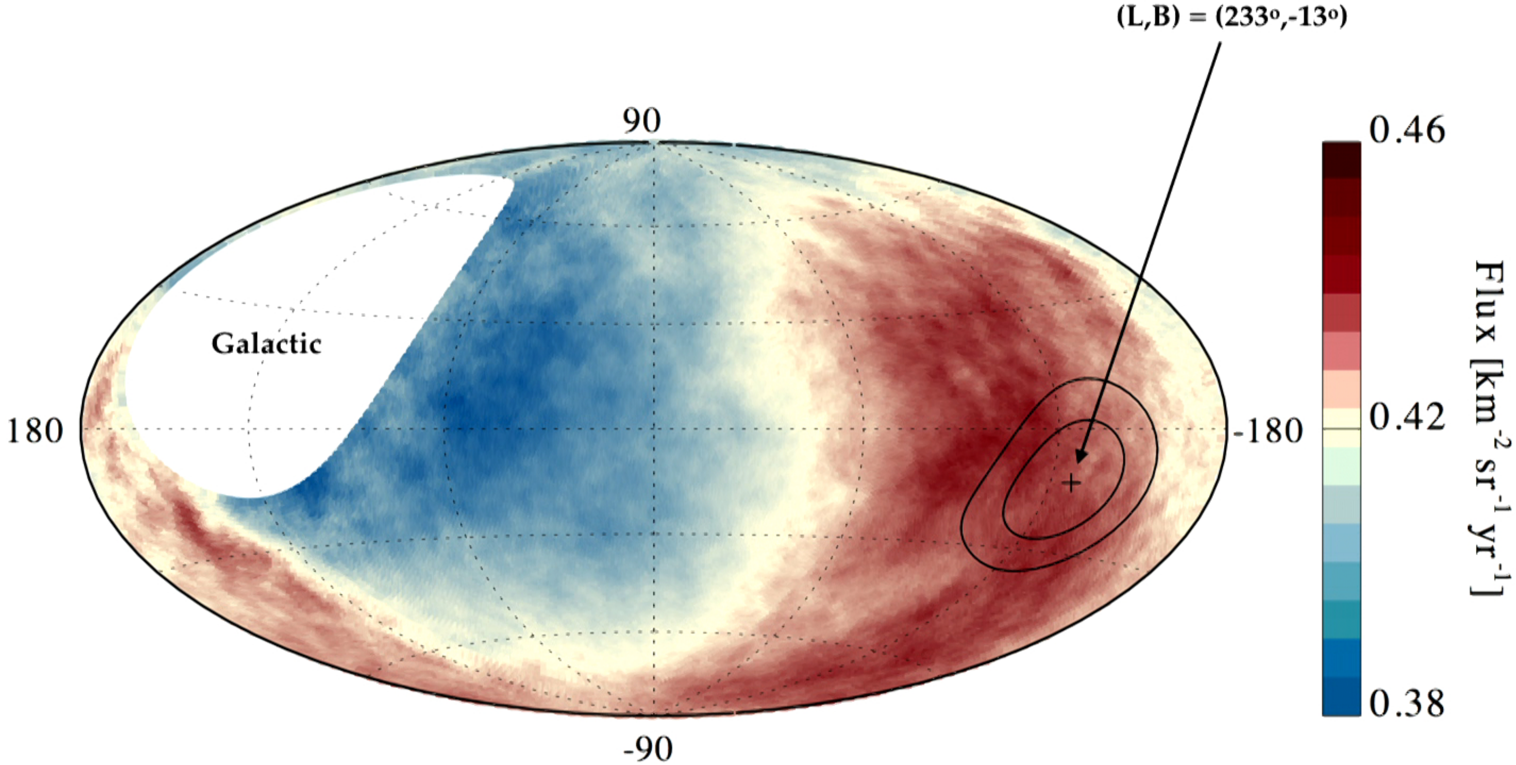

- Broad 45° top-hat beam applied
- Dipole maximum is about 125° away from the galactic center

Reconstruction of the 3D dipole

Science 57 (2017) 1266

Components parallel and perpendicular to the Earth rotation axis:

$$d_z \approx \frac{b_\varphi}{\cos \ell_{obs} \langle \sin \theta \rangle} \qquad d_\perp \approx \frac{r_\alpha}{\langle \cos \delta \rangle}$$

Right ascension and declination:

$$\alpha_d = \varphi_\alpha \qquad \tan \delta_d = \frac{d_z}{d_\perp}$$

E>8 EeV

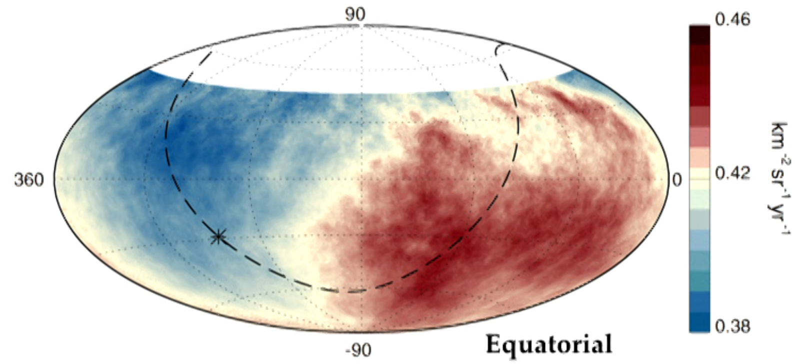

Equatorial

Energy (EeV)	Dipole component d_z	Dipole component $d_\perp$	Dipole amplitude d	Dipole declination δ_d (°)	Dipole right ascension α_d (°)
4 to 8	−0.024 ± 0.009	$0.006^{+0.007}_{-0.003}$	$0.025^{+0.010}_{-0.007}$	-75^{+17}_{-8}	80 ± 60
≥8	−0.026 ± 0.015	$0.060^{+0.011}_{-0.010}$	$0.065^{+0.013}_{-0.009}$	-24^{+12}_{-13}	100 ± 10

- **Reconstruction assumes the dipole is the dominant component of the anisotropy**
- **Analysis of the power spectrum gives support to this hypothesis**

Power spectrum

JCAP 06 (2017) 026

- Further evidence of the dominance of the dipole coming from the power spectrum

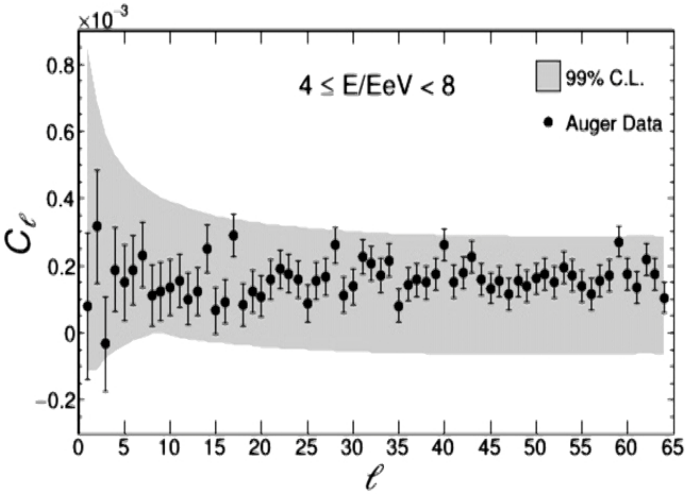

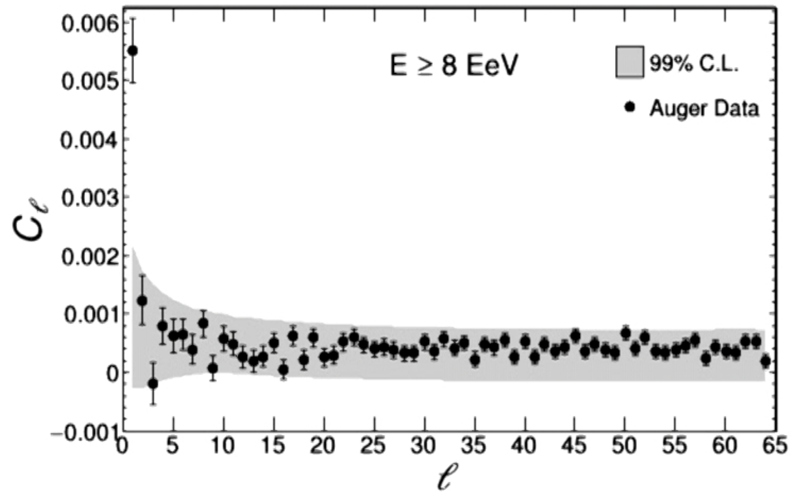

- Slightly different data sample:
  - 01-01-2004 to 12-31-2013
  - Tight fiducial quality trigger

Time evolution of the signal

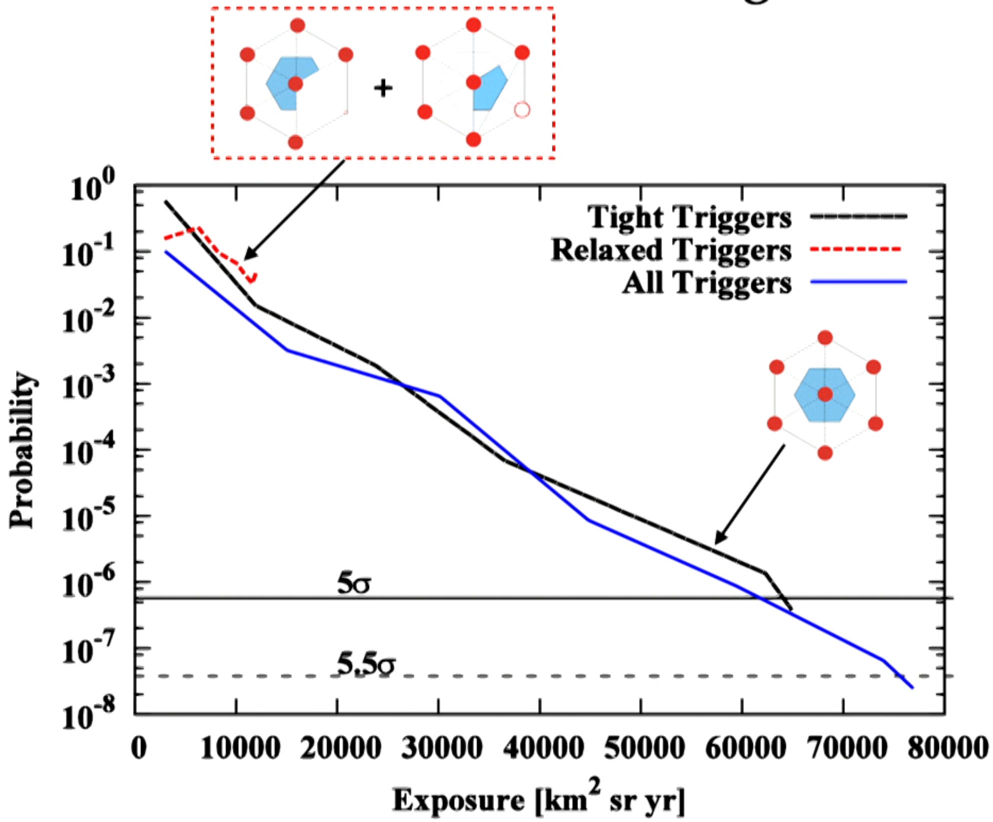

- Steady drop of the chance probability as data is accumulated

Final sky map: galactic coordinates

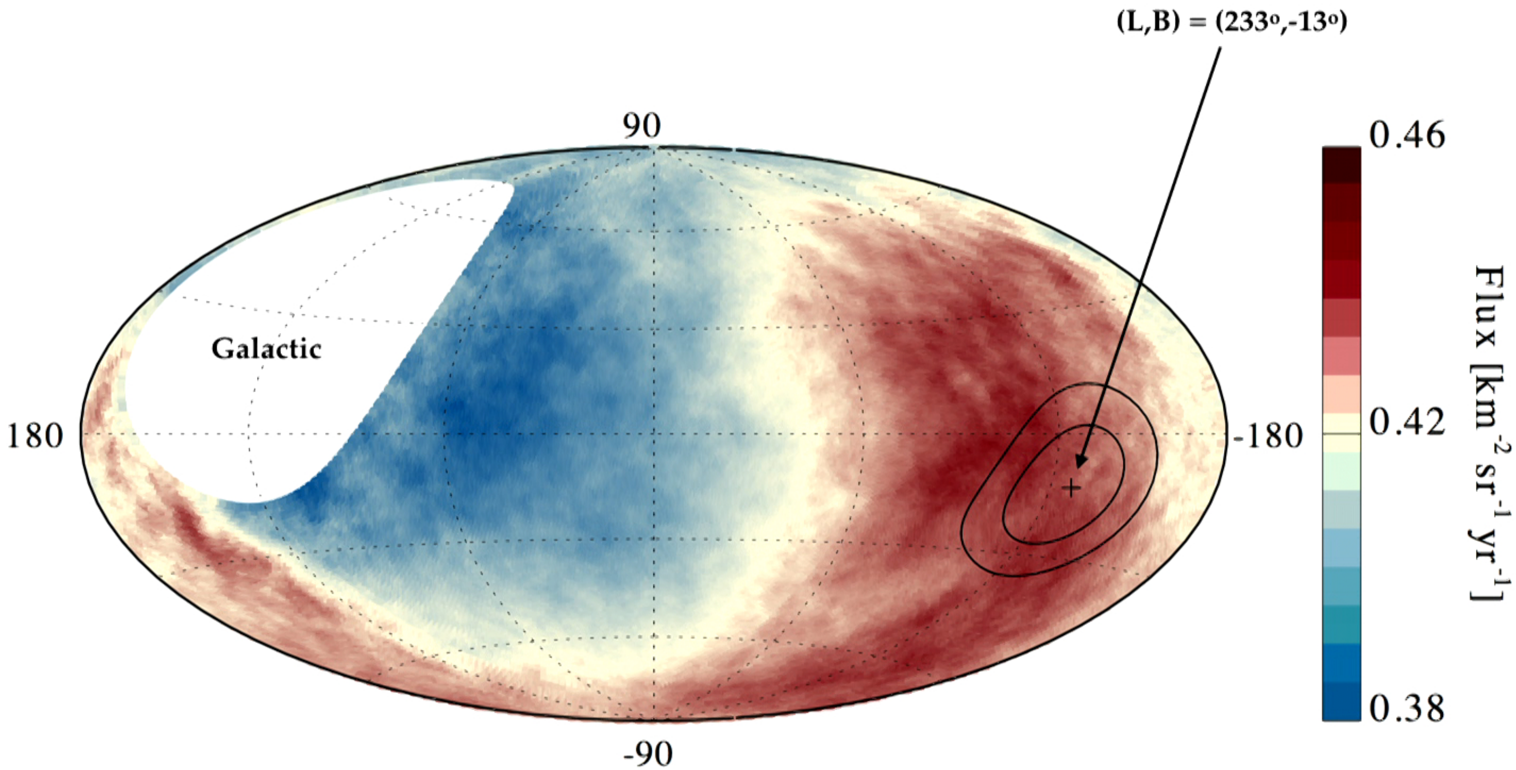

- Broad 45° top-hat beam applied
- Dipole maximum is about 125° away from the galactic center

Final sky maps: EQU, GAL and SGAL coordinates

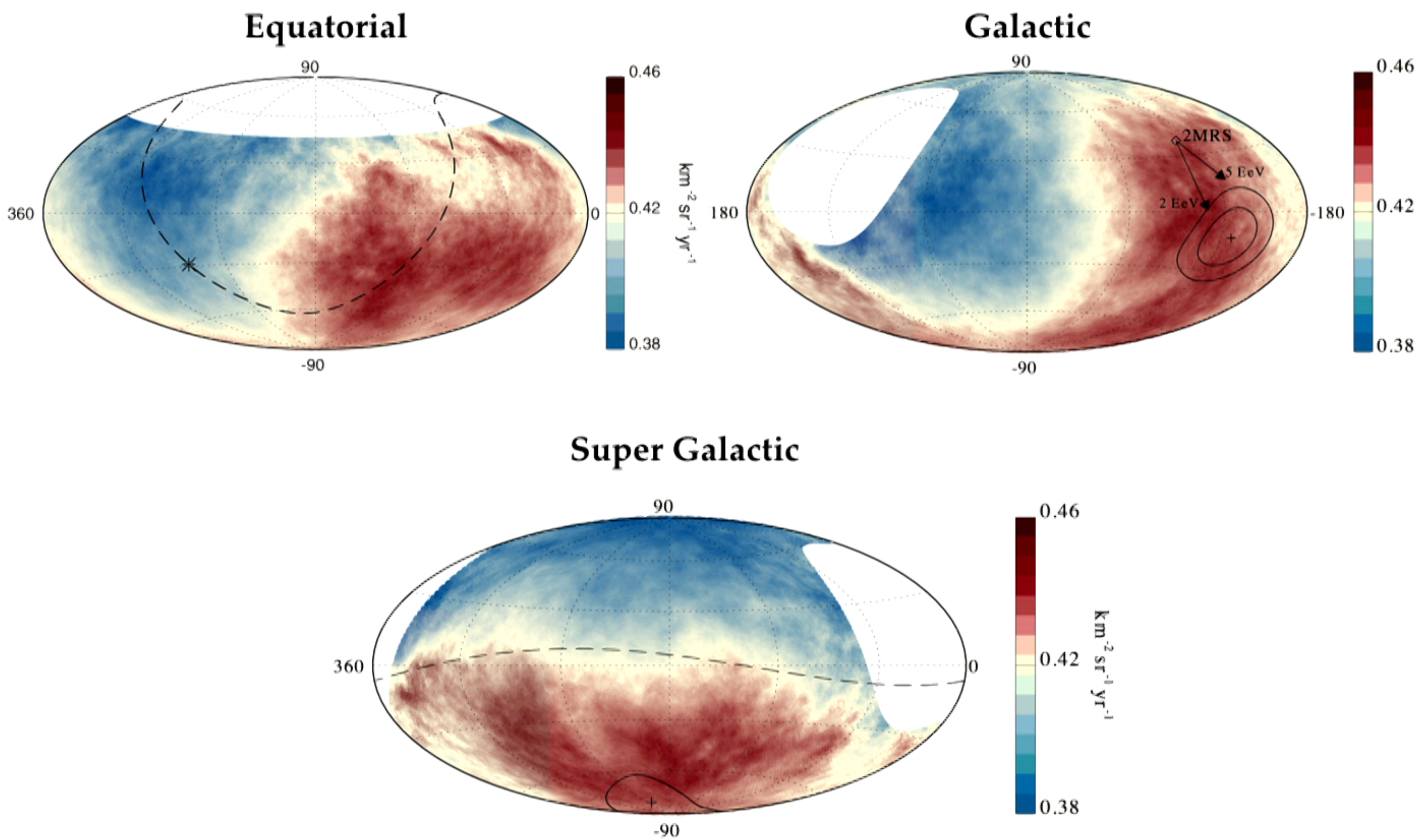

Cosmological Compton-Getting effect

Planck CMB dipole:

Eppur si muove!

$(\ell, b) = (264°, 48°)$

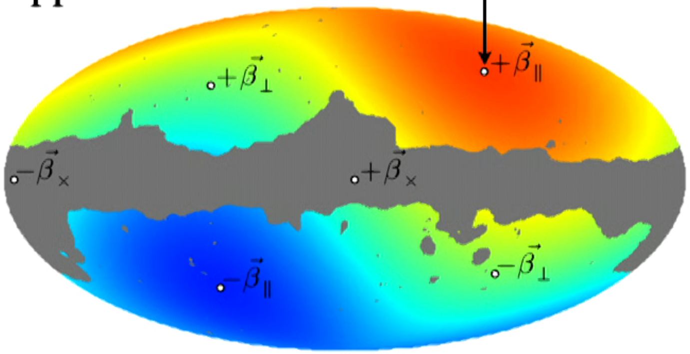

$v = 384\,\mathrm{km\ s^{-1}} \pm 78\,\mathrm{km\ s^{-1}}(\mathrm{stat}) \pm 115\,\mathrm{km\ s^{-1}}(\mathrm{syst})$

order 10^{-3} effect

- **Assumption: sources of UHECRs are distributed at cosmological distances**
- **Movement of the solar system barycenter in the CMB rest frame should also induce a dipolar anisotropy in the flux of UHECR aligned with the CMB dipole**

$$J'(E') \simeq J(E)\left[1 - \frac{\mathbf{u}\cdot\mathbf{p}}{p}\left(2 - \frac{\mathrm{d}\ln J}{\mathrm{d}\ln E'}\right)\right]$$

Spectra in CMB (unprimed) and observer (primed) frames

- **Amplitude is below 1% for a spectrum E-2.7 above the ankle:**

$$A_{CCG} = \frac{J_{max} - J_{min}}{J_{max} + J_{min}} = \left(2 - \frac{\mathrm{d}\ln J}{\mathrm{d}\ln E'}\right) \simeq 0.6\%$$

- **3-sigma detection would need ~10^6 events**

Compton & Getting, Phys. Rev. 47 (1935) 817
Phys. Lett. B 640 (2006) 225–229

Is it consistent with local matter distribution and mag. fields?

2MASS Redshift Survey (2MRS)

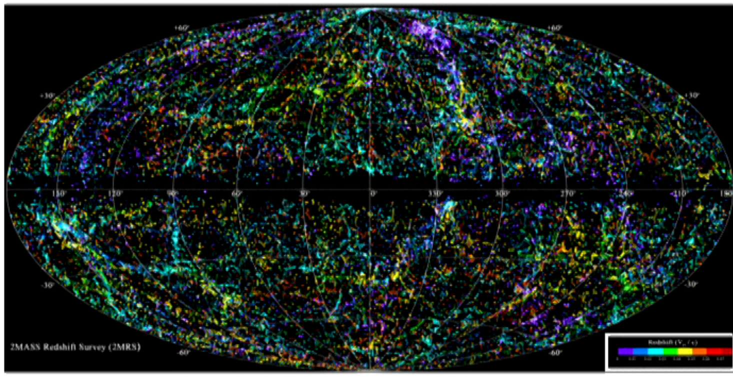

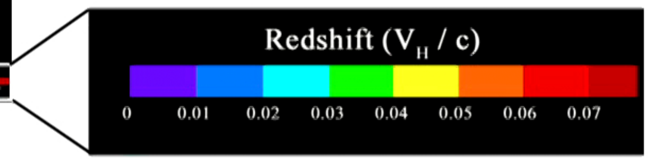

- 91% of sky coverage
- 97.6% of completeness
- ~ 43k galaxies
- $K_s \leq 11.75$ mag
- D < 300 Mpc

+

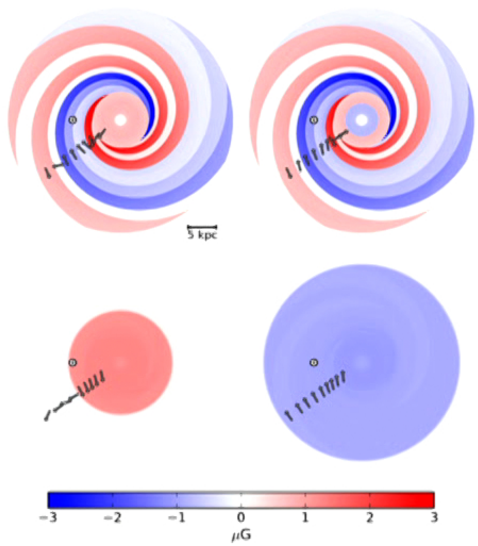

- 3 components: spiral disk + toroidal at halo + poloidal
- Rotation measures → $\propto \int_{los} d\ell \, n_e(\mathbf{r}) B_{||}(\mathbf{r})$
- Synchrotron emission (WMAP) → $\propto \int_{los} d\ell \, n_{cre}(\mathbf{r}) B_{\perp}(\mathbf{r})$

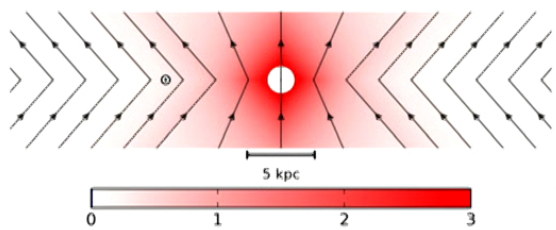

RJ & GF, Ap.J. 757, 14 (2012)

40

Is it consistent with local matter distribution and mag. fields?

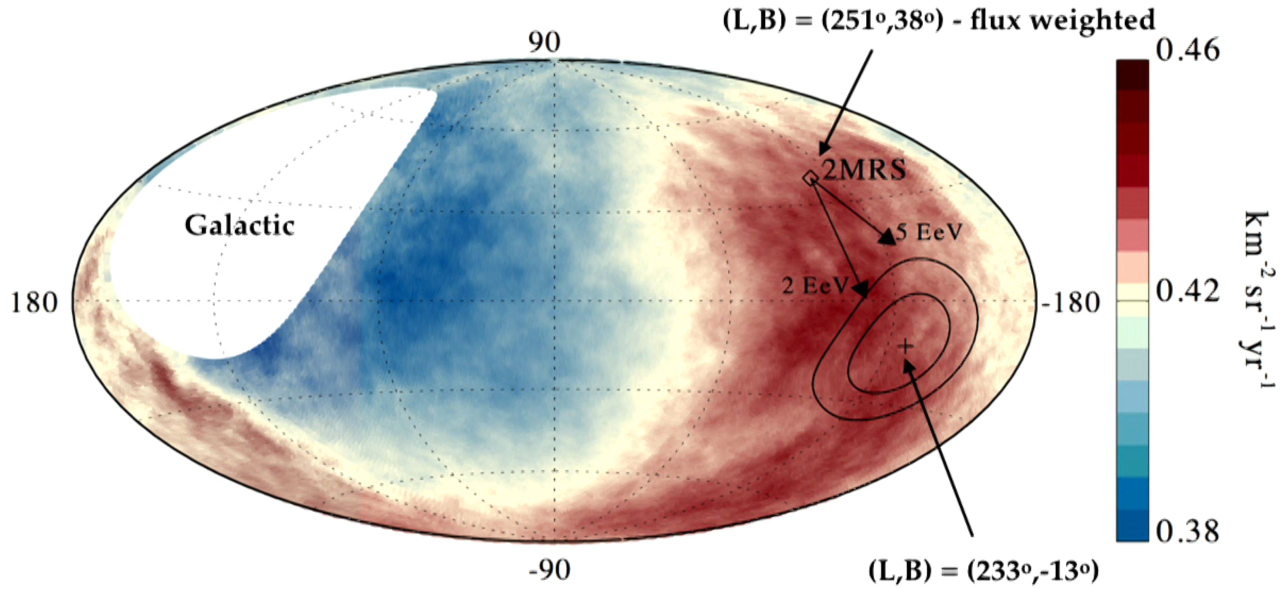

- Two rigidities shown: E/Z = 2, 5 EeV representing the typical Z values (1.7-5) inferred from X_{max} at 10 EeV
- Typically, up to 5-20% (around 10 EeV) dipole amplitudes can be obtained from local inhomogeneities and deflection in magnetic fields depending on CR composition

Summary

- **Anisotropy searches performed at all angular scales: small, intermediate and large**
- **Indications of anisotropy at the 4σ level from a maximum log-likelihood analysis based on starburst galaxy model**
- **Observation of a dipolar large scale pattern at more than 5σ level above 8 EeV**
- **Direction of the dipole (~125° away from GC) is better explained if the bulk of these UHECRs are extragalactic in origin**
- **No statistically significant sign of anisotropy seen so far at lower energies (around and below the ankle)**